(12) INTERNATIONAL APPLICATION PUBLISHED UNDER THE PATENT COOPERATION TREATY (PCT)

(19) World Intellectual Property Organization
International Bureau

(43) International Publication Date
29 October 2015 (29.10.2015)

WIPO | PCT

(10) International Publication Number
WO 2015/162130 A1

(51) International Patent Classification:
C07H 19/052 (2006.01) *C12Q 1/68* (2006.01)

(21) International Application Number:
PCT/EP2015/058600

(22) International Filing Date:
21 April 2015 (21.04.2015)

(25) Filing Language: English

(26) Publication Language: English

(30) Priority Data:
14001463.0 24 April 2014 (24.04.2014) EP

(71) Applicant: **ETH ZURICH** [CH/CH]; Raemistrasse 101 / ETH transfer, CH-8092 Zurich (CH).

(72) Inventors: **STURLA, Shana**; Dolderstrasse 18, CH-8032 Zürich (CH). **TRANTAKIS, Ioannis**; Neptunstrasse 59, CH-8032 Zürich (CH). **DAHLMANN, Heidi**; Friedrich-strasse 20, CH-8051 Zürich (CH).

(81) Designated States *(unless otherwise indicated, for every kind of national protection available)*: AE, AG, AL, AM, AO, AT, AU, AZ, BA, BB, BG, BH, BN, BR, BW, BY, BZ, CA, CH, CL, CN, CO, CR, CU, CZ, DE, DK, DM, DO, DZ, EC, EE, EG, ES, FI, GB, GD, GE, GH, GM, GT, HN, HR, HU, ID, IL, IN, IR, IS, JP, KE, KG, KN, KP, KR, KZ, LA, LC, LK, LR, LS, LU, LY, MA, MD, ME, MG, MK, MN, MW, MX, MY, MZ, NA, NG, NI, NO, NZ, OM, PA, PE, PG, PH, PL, PT, QA, RO, RS, RU, RW, SA, SC, SD, SE, SG, SK, SL, SM, ST, SV, SY, TH, TJ, TM, TN, TR, TT, TZ, UA, UG, US, UZ, VC, VN, ZA, ZM, ZW.

(84) Designated States *(unless otherwise indicated, for every kind of regional protection available)*: ARIPO (BW, GH, GM, KE, LR, LS, MW, MZ, NA, RW, SD, SL, ST, SZ, TZ, UG, ZM, ZW), Eurasian (AM, AZ, BY, KG, KZ, RU, TJ, TM), European (AL, AT, BE, BG, CH, CY, CZ, DE, DK, EE, ES, FI, FR, GB, GR, HR, HU, IE, IS, IT, LT, LU, LV, MC, MK, MT, NL, NO, PL, PT, RO, RS, SE, SI, SK, SM, TR), OAPI (BF, BJ, CF, CG, CI, CM, GA, GN, GQ, GW, KM, ML, MR, NE, SN, TD, TG).

Published:

— *with international search report (Art. 21(3))*

WO 2015/162130 A1

(54) Title: BASE-MODIFIED-NUCLEOSIDE ANALOGS FOR THE DETECTION OF O^6-ALKYL GUANINE

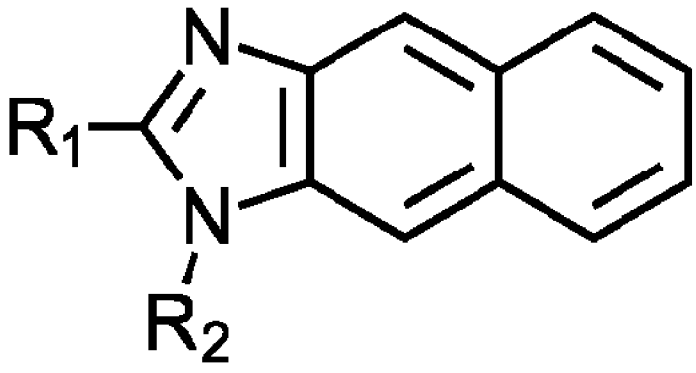

(57) Abstract: The present disclosure provides novel compounds containing a base- modified nucleoside of formula and methods for detecting the presence of guanine in a nucleic acid and for isolating O^6-alkyl guanine comprising nucleic acid. The disclosure is based on base-modified-nucleoside analogs that form stable base pairs with O^6-alkyl guanine.

Title:

BASE-MODIFIED-NUCLEOSIDE ANALOGS FOR THE DETECTION OF O^6-ALKYL GUANINE

FIELD OF THE INVENTION

The present disclosure provides novel compounds and methods for detecting the presence of O^6-alkyl guanine in a nucleic acid and for isolating O^6-alkyl guanine comprising nucleic acid. The disclosure is based on base-modified-nucleoside analogs that form stable base pairs with O^6-alkyl guanine.

BACKGROUND OF THE INVENTION

In our daily life we are constantly exposed to genotoxic chemicals that may interact with cellular DNA, become covalently bound, and generate products called DNA adducts. If DNA adducts persist and evade repair they can lead to mutations in cell-cycle regulatory genes that may cause uncontrolled cell division leading to cancer. Therefore DNA adduct formation is considered one of the key events in tumor initiation during chemical carcinogenesis[1-3]. Levels of DNA adducts represent the amount of carcinogen absorbed by the body, escaped detoxification, encountered a critical cellular macromolecule (DNA) and has not been repaired. Therefore, DNA adducts serve as chemical-specific biomarkers of biologically significant exposure to genotoxins and individual susceptibility to carcinogenesis[4,5]. Similarly, some of the most commonly used cancer therapeutics work by forming DNA adducts that trigger cell death in rapidly dividing target cancer cells, and DNA adducts serve in this situation as chemical biomarkers of drug sensitivity. As a result, these chemical biomarkers are measured in cancer epidemiology population studies and in chemotherapy clinical trials. The anticipated outcome of ongoing research involving the detection of DNA adducts as chemical biomarkers is personalized medicine or wellness strategies for cancer prevention and therapy that rely on accessible detection technologies.

A current difficulty in detecting DNA adducts is that they are formed at exceedingly low levels. The ability of DNA lesions to induce toxicity depends on their chemical structure, abundance of formation and propensity to be recognized by specialized DNA repair proteins, and their positions within the genome[8,9]. With respect to genome positioning, local DNA sequence context influences the rate of DNA adduct formation,

repair and mispairing potency[10]. Furthermore, the location of a DNA lesion within the gene will determine whether it results in mutations influencing the structure and function of the corresponding protein. Current DNA adduct analysis techniques, including ^{32}P-postlabeling, immunoassay, fluorescence spectroscopy, and mass spectrometry[11], have been largely focused on the detection of monomeric nucleoside or nucleotide adducts without giving information about the sequence context of the lesion. Therefore new approaches for addressing low-abundance adducts in a sequence-specific manner are needed.

SUMMARY OF THE INVENTION

A first aspect of the disclosure provides an oligonucleotide comprising at least one base-modified-nucleotide analog wherein the base-modified-nucleotide comprises the following structure:

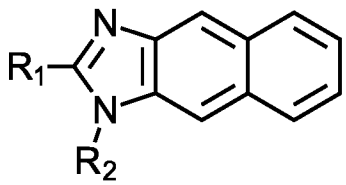

wherein R1 is selected from OH or H; and R2 is selected from a deoxyribose moiety of a polynucleotide, a ribose moiety of a polynucleotide, and a nucleic acid backbone mimic moiety. Preferably R1 is OH and R2 is selected from a ribose moiety, a deoxyribose moiety, and a nucleic acid backbone mimic moiety or R1 is H and R2 is selected from a deoxyribose moiety and a nucleic acid backbone mimic moiety. Preferably R1 is selected from OH or H and R2 is a deoxyribose moiety of a polynucleotide. Preferably, R1 is OH.

Preferably, said oligonucleotide is immobilized to a solid surface, more preferably a nanoparticle, more preferably a gold nanoparticle. A further aspect of the disclosure provides a kit of parts comprising the oligonucleotides and a solid substrate, preferably particles, more preferably gold nanoparticles. A further aspect provides the use of said oligonucleotides for detecting the presence of *O*^{6}-alkyl guanine, in particular the presence of *O*^{6}-alkyl guanine in a target polynucleotide.

A further aspect of the disclosure provides a base-modified-nucleoside analog having the following structure:

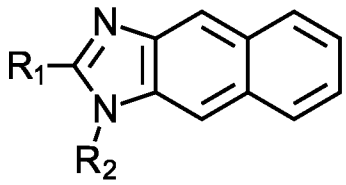

wherein R1 is OH and R2 is selected from a ribose moiety, a deoxyribose moiety, and a nucleic acid backbone mimic moiety or R1 is H and R2 is selected from a deoxyribose moiety and a nucleic acid backbone mimic moiety. Preferably, R1 is OH.

Preferably, the base modified nucleoside analog has the following structure:

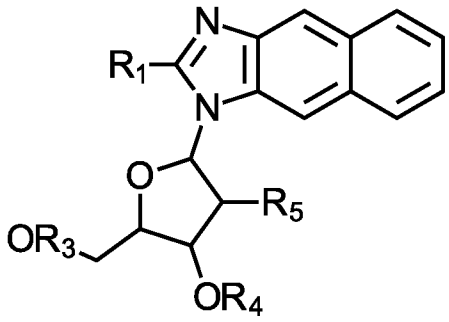

wherein R3 is selected from H, phosphorothioate monophosphate, (PO_3), $(PO_3)_2$, $(PO_3)_3$, and a protective group for a hydroxyl group for synthesis of nucleic acid, preferably R3 is H and

R4 is selected from H, a protective group for a hydroxyl group for synthesis of nucleic acid, a phosphate group, a phosphate group protected with a protective group for synthesis of nucleic acid, or -P(R7)R8 [where R7 and R8 are identical or different, and each represent a hydroxyl group, a hydroxyl group protected with a protective group for synthesis of nucleic acid, a mercapto group, a mercapto group protected with a protective group for synthesis of nucleic acid, an amino group, an alkoxy group having 1 to 5 carbon atoms, an alkylthio group having 1 to 5 carbon atoms, a cyanoalkoxy group having 1 to 6 carbon atoms, or a primary or secondary amine substituted by an alkyl group having 1 to 5 carbon atoms, preferably R4 is H, and

R5 is selected from H, OH, O-alkyl(Cl-C6), F, CI, NH2, CN, SH, and a 2'- 4' bridge locking the sugar in the C3 endo configuration, wherein R5 is not OH when R1 is H; preferably R5 is H.

A further aspect of the disclosure provides a method for detecting the presence of O^6-alkyl guanine in a target polynucleotide,
said method comprising a) contacting the target polynucleotide (or a sample comprising said target polynucleotide) with a first oligonucleotide that is complementary to said polynucleotide such that said target polynucleotide and said first oligonucleotide form a target duplex wherein
said oligonucleotide comprises at least one base-modified-nucleotide analog comprising the following structure:

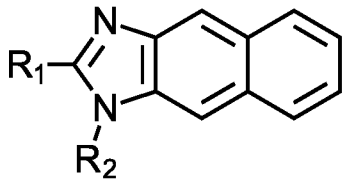

wherein R1 is selected from OH or H, preferably OH; and R2 is selected from a deoxyribose moiety of a polynucleotide, a ribose moiety of a polynucleotide, and a nucleic acid backbone mimic moiety and b) measuring the formation of said duplex. Preferably, said oligonucleotide is immobilized to a solid surface, more preferably a nanoparticle, more preferably a gold nanoparticle.

Preferably the method further comprises contacting the target polynucleotide with a second oligonucleotide that is complementary to said polynucleotide such that said polynucleotide can simultaneously hybridize to both the first and second oligonucleotides forming a duplex and b) measuring the formation of said duplex.

Preferably the method alternatively comprises contacting said target polynucleotide with a second oligonucleotide that is complementary to said first oligonucleotide such that said second oligonucleotide competes with the target polynucleotide for binding to the first oligonucleotide (comprising the base-modified nucleotide analog).

A further aspect of the disclosure provides a method for isolating an O^6-alkyl guanine containing target polynucleotide, said method comprising a) contacting a nucleic acid containing sample with an oligonucleotide that is complementary to said target polynucleotide such that said target polynucleotide and said oligonucleotide form a target duplex, said oligonucleotide comprises at least one base-modified-nucleotide analog comprising the following structure:

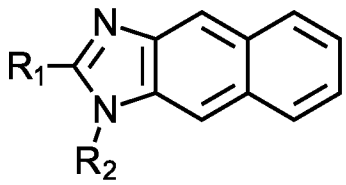

wherein R1 is selected from OH or H, preferably OH; and R2 is selected from a deoxyribose moiety of a polynucleotide, a ribose moiety of a polynucleotide, and a nucleic acid backbone mimic moiety and b) isolating said target duplex. Preferably said oligonucleotide is coupled to a purification label or a solid substrate and the target duplex is isolated via the purification label or solid substrate.

Preferably, O^6-alkyl guanine is O^6-methyl guanine.

BRIEF DESCRIPTION OF THE DRAWINGS

Figure 1. A) *O*^{6}-methyl-G and *O*^{6}-benzyl-G. B) Hydrophophobic nucleoside analogs designed to pair opposite *O*^{6}-alkyl-G lesions. dR = deoxyribose.

Figure 2: Statistical analysis of $\Delta G_{CF}°$ of duplex melting (Table 2). Error bars indicate 95% confidence intervals. Analog:target pairs that do not differ significantly (i.e, pairs in which $p > 0.05$) according to the Games-Howell test are denoted (-).

Figure 3. Fluorescence emission spectra of 5 µM dsDNA in PBS buffer containing nucleoside analogs ExBIM and ExBenzi excited at 250 nm. A) ExBIM base paired opposite G, *O*^{6}-MeG, and THF B) Exbenzi base paired opposite G, *O*^{6}-MeG, and THF.

Figure 4. SCHEME 1. Synthesis of nucleoside analog phosporamidites. a) urea, microwave irradiation. b) formic acid, EtOH, 75 °C. c) **9**, NaH, THF, 25 °C. d) NaH, MeOH:THF (1:9), 25 °C. e) DMT·BF_4, Li_2CO_3, Hunig's base, THF, 25 °C. f) **12**, Hunig's base, DCM, 25 °C.

Figure 5: A) The synthetic nucleoside ExBIM forms stable base pairs with O^6-meG. B) AuNP probes: AuNPs tail-to tail functionalized with two sets of oligonucleotides, with ExBIM incorporated into one set, indicated with terminal P. Target binding leads to NP aggregation and red to purple color change. The purple solution indicates the adduct.

Figure 6: Comparison of UV-Vis spectra of a mixture of AuNP probes before and after treatment with a complementary target oligonucleotide

Figure 7: A) Dependence of absorbance ratios on temperature of aggregates formed from target mixtures (20 nM of each G and irrelevant target) supplemented with either O^6-meG- (20 nM final concentration) or G-containing targets (40 nM final concentration). An aggregate solution formed from the initial mixture (blank) served as a control. Data points indicate mean±SD from three independent experiments. B) Differential absorbance ratios between aggregates formed from target mixture (20 nM of each G and irrelevant target) supplemented with O^6-meG-containing target (20 nM final concentration) and aggregates formed from target mixture supplemented with G-containing target (40 nM final concentration).

Figure 8. A) Linear plot of absorbance ratios (700/530 nm) versus relative O^6-meG target concentration ([O^6-meG]/[total target]). B) Linear plot of absorbance ratios (700/530 nm) versus relative O^6-meG target concentration ([O^6-meG]/[G]). Values are mean±SD from three independent experiments.

DE TAILED DESCRIPTION OF THE DISCLOSED EMBODIMENTS

While there are a large number of putative DNA adduct targets that may be of interest to measure in an individual, it has been widely reported that low levels of aberrant methylation of DNA are frequently observed in human populations. The methylated DNA bases most commonly found are N^7-methylguanine (N^7-meG) and O^6-methylguanine (O^6-meG), detected in DNA isolated from blood lymphocytes or leukocytes, gastrointestinal tissues, lung, urinary bladder placenta, and other human tissues[12-16]. These aberrant bases are believed to represent DNA damage caused by methylating agents of dietary, environmental, or endogenous origin. Of these two lesions, it is the presence of O^6-meG in human DNA that is considered to be of particular toxicological relevance because it is strongly mutagenic[17-19], causing G→A mutations via a direct miscoding mechanism, and appears to be of major importance

in the development of tumors in experimental animals treated with methylating carcinogens[20,21]. The observation[22-24] of a high frequency of G→A transition mutations in the K-*ras* or *p53* genes of human colon and lung tumors lacking O^6-meG–DNA methyltransferase (MGMT), an enzyme that specifically repairs O^6-meG in DNA[25], implies the etiologic involvement of O^6-meG in colon and lung carcinogenesis, underlining the need to detect its presence in human biological samples. Despite the recognized significance of the presence of O^6-meG in human DNA, there are limited strategies for measuring its occurrence in human populations [26]. Radiolabelling, immunohistochemistry, or HPLC coupled with MS or electrochemical detection are useful for detecting low-abundance O^6-alkyl-G DNA lesions in biological samples; however, these methods involve time- and labor-intensive sample preparation and analysis(de Groot et al., 1994; Dennehy and Loeppky, 2005; Georgiadis et al., 2011; Huh et al., 1989; Kang et al., 1992; Yang et al., 2002). (de Groot et al., 1994; Dennehy and Loeppky, 2005; Georgiadis et al., 2011; Huh et al., 1989; Kang et al., 1992; Yang et al., 2002) and are not able to target DNA adducts in specific sequence contexts. Sequence-specific detection of DNA is typically carried out by hybridizing oligonucleotide probes with complementary target DNA. This method is used for example in microarrays or DNA chips, which have become ubiquitous in biological and biomedical research.(Gresham, 2011; Nazar and Robb, 2012; Sealfon and Chu, 2011; Wang et al., 1998; Wang and Li, 2011) Hybridization probes containing nucleoside analogs that selectively interact with specific DNA lesions as opposed to non-damaged DNA have been developed to monitor biochemical transformations such as abasic site formation, DNA repair, and translesion and postlesion DNA synthesis on damaged DNA substrates.(Gahlon et al., 2013; McCullough et al., 1997; Rachofsky et al., 2001; Roday et al., 2008; Shipova and Gates, 2005; Stivers, 1998) The nucleoside analogs utilized in these hybridization probes often contain fluorescent conjugated ring systems that facilitate spectroscopic detection; such nucleoside analogs have been incorporated into hybridization probes for 8-oxo-G and abasic sites.(Greco et al., 2009; Greco and Tor, 2005; Nasr et al., 2009; Stivers, 1998; Wilhelmsson, 2010) Other nucleoside analogs have been designed to chemically react with the target lesion; for example, a hybridization probe that specifically transfers an alkynylated enone to O^6-meG but not to G was recently reported. The alkynylated O^6-

meG can subsequently be labelled with a fluorescent reporter or biotin group via click chemistry to enable detection of the lesion in duplex DNA.(Onizuka et al., 2012)

An alternative type of hybridization probe for site-specific detection of O6-Me-G contains hydrophobic nucleoside analogs (Benzi, BIM, Peri, and Per, Figure 1B) that form more stable base pairs opposite O^6-alkyl-G lesions than opposite non-damaged G, A, T, and C.(Gahlon and Sturla, 2013b; Gong and Sturla, 2007)

The present disclosure provides nucleoside analogs Exbenzi and ExBIM for the detection of O^6-alkyl guanine (Figure 1B). The thermal stabilities of duplexes containing ExBenzi and ExBIM paired opposite G, O^6-Me-G, O^6-Bn-G, and a model abasic site (THF) as a control were evaluated according to their free energies of duplex melting, which were derived from UV-absorbance melting curves. The oligonucleotide probe containing Exbenzi was more selective for O^6-alkyl-G vs G strands than the previously described Per nucleoside. The larger nucleobases Exbenzi and ExBIM better stabilized the ends of DNA than their smaller counterparts Benzi and BIM (Table 3). Quantum yields of BIM, Benzi, ExBIM, and Exbenzi nucleosides were determined. When ssDNA was hybridized to dsDNA, the fluorescent signal was quenched (10 fold with ExBIM, 20 fold with Exbenzi). However, a trend for higher fluorescence intensity was observed when nucleoside analogs were paired with O^6-Me-G vs. G or THF (Figure 3).

Accordingly, the disclosure provides base-modified-nucleoside analogs and oligonucleotides comprising said nucleoside analogs for detecting the presence of O^6-alkyl guanine or for isolating a nucleic acid containing O^6-alkyl guanine. In preferred embodiments, O^6-alkyl guanine is O^6-methyl guanine.

Preferably, a base-modified-nucleoside analog as disclosed herein has the following structure:

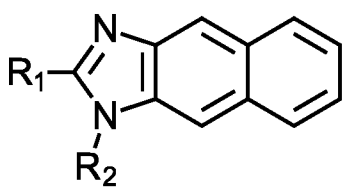

wherein R1 is OH or H and R2 is selected from a ribose moiety, a deoxyribose moiety, and a nucleic acid backbone mimic moiety. Preferably R1 is OH and R2 is selected from a ribose moiety, a deoxyribose moiety, and a nucleic acid backbone mimic moiety or R1 is H and R2 is selected from a deoxyribose moiety and a nucleic acid backbone mimic moiety. Preferably R1 is OH.
These nucleoside analogs are referred to herein as ExBIM (R1 is H) and Exbenzi (R1 is OH).

The sugar moiety of the nucleosides may contain additional natural and/or non-natural modifications and/or substitutions, including stabilizing modifications/substitutions and purification or detection labels. The base-modified-nucleosides also include mono-, di-, and tri-phosphate nucleosides, i.e., "nucleotides". Additional modifications are known to the skilled person. EP0,302,175 describes modification of nucleotides at the 5' or 3' end, as well as modification of the phosphate moiety and US5446137 describes nucleotides that are substituted at the 4' position of the sugar moiety. Locked Nucleic Acid derivatives are also encompassed by the disclosure. LNAs are modified nucleotides or ribonucleotides that contain an extra bridge between the 2' and 4' carbons of the ribose sugar moiety resulting in a "locked" conformation, and/or bicyclic structure.

Nucleic acid backbone mimic moieties are well-known in the art and include, e.g. GNAs, PNA, and TNAs. GNA (glycol nucleic acid) comprises a backbone of glycols linked by phosphodiester bonds. PNA (peptide nucleic acid) comprises, N-(2-aminoethyl)-glycine lined by peptide bonds. TNA (threose nucleic acid) comprises a backbone of threose sugars linked by phosphodiester bonds.

The nucleosides may also include protective groups, e.g., protective groups for the synthesis of nucleic acid. Protective group refers to a chemical group that changes a functional group so as to disguise the chemical reactivity of the functional group and prevent it from undesirably reacting during reactions occurring at other sites on the compound. Suitable protecting groups include phthalyl, carbobenzyloxy, benzyl, benzoyl, trityl, monomethoxytrityl, dimethoxytrityl (DMT), acetyl, trifluoroacetyl,

trimethylsilyl, t-butyl(dimethyl)silyl, t-butyl(diphenyl)silyl, carbonate, 2-trimethylsilylethyl, methoxymethyl, 2-methoxyethoxymethyl and dihydropyranyl groups.

In preferred embodiments, the base-modified-nucleoside analog has the following structure:

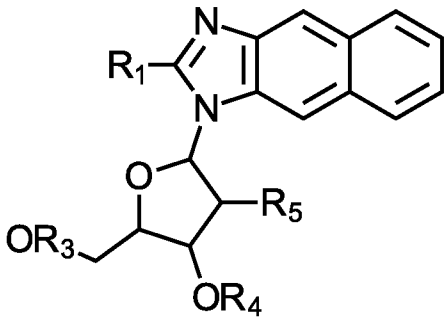

wherein R1 is selected from OH or H, preferably R1 is OH;
R3 is selected from H, phosphorothioate monophosphate, (PO_3), $(PO_3)_2$, $(PO_3)_3$ and a protective group for a hydroxyl group for synthesis of nucleic acid,
R4 is selected from H, a protective group for a hydroxyl group for synthesis of nucleic acid, a phosphate group, a phosphate group protected with a protective group for synthesis of nucleic acid, or -P(R7)R8 [where R7 and R8 are identical or different, and each represent a hydroxyl group, a hydroxyl group protected with a protective group for synthesis of nucleic acid, a mercapto group, a mercapto group protected with a protective group for synthesis of nucleic acid, an amino group, an alkoxy group having 1 to 5 carbon atoms, an alkylthio group having 1 to 5 carbon atoms, a cyanoalkoxy group having 1 to 6 carbon atoms, or a primary or secondary amine substituted by an alkyl group having 1 to 5 carbon atoms], and
R5 is selected from H, OH, O-alkyl(Cl-C6), F, CI, NH2, CN, SH, and a 2'- 4' bridge locking the sugar in the C3 endo configuration.
Preferably, R5 is not OH when R1 is H. Preferably R5 is H.

The base-modified-nucleoside analogs disclosed herein and the oligonucleotides comprising base-modified-nucleotide analogs disclosed herein (referred herein collectively as “the compounds of the disclosure”) may be used to detect the presence

of O^6-alkyl guanine in a sample. The compounds of the disclosure may also be used to isolate or enrich for O^6-alkyl guanine. Preferably, the O^6-alkyl guanine is present as a unit of a polynucleotide, i.e., the compounds detect the presence of O^6-alkyl guanine in a nucleic acid sequence. A polynucleotide comprises at least two nucleotide monomers, preferably at least 3, 4, 5 or more nucleotide monomers. The terms "polynucleotide" and "nucleic acid sequence" are used interchangeably herein.

O^6-alkyl guanine can be detected in or isolated from any sample that contains or is suspected of containing nucleic acid. Samples include water, food, cells, organisms, tissue, stool, and biological fluids (e.g., plasma, serum, urine, tears, saliva, spinal fluid or lymph fluids). In some embodiments, the samples are obtained from individuals at risk or suspected of being at risk of having or developing a hyperproliferative disorder, e.g., tumor, cancer, neoplastic tissue. In some embodiments, the individuals have been exposed to or are suspected of being exposed to a carcinogen, e.g., radiation, a carcinogen in cigarettes, etc. In some embodiments, the individual is undergoing chemotherapy. The nucleic acid may be RNA or DNA or fragments thereof. Preferably, the nucleic acid is DNA.

In preferred embodiment, the compounds of the disclosure are used to detect the presence of O^6-alkyl guanine in a target polynucleotide or to enrich or isolate for a O^6-alkyl guanine containing target polynucleotide. Accordingly, one preferred object of the disclosure is to provide compounds that target DNA adducts in sequence specific context. Preferably, oligonucleotides are designed to hybridize with nucleic acid susceptible to damage or to nucleic acid whose damage leads to harmful effects. Preferred target polynucleotides include oncogenes (e.g., K-ras and p53). The target sequence may comprise nucleic acid fragments, e.g., fragments that comprise mutational "hotspots". Fragments having a known sequence can be prepared by, e.g., digesting a nucleic acid sample with one or more restriction enzymes.

In addition to detecting O^6-alkyl guanine, the disclosed nucleotide analogs are also used as intermediates for production of oligonucleotides. Accordingly, the disclosure provides an oligonucleotide comprising at least one base-modified-nucleotide analog as disclosed herein. Preferably, an oligonucleotide is provided comprising at least one

base-modified-nucleotide analog wherein the base-modified-nucleotide comprises the following structure:

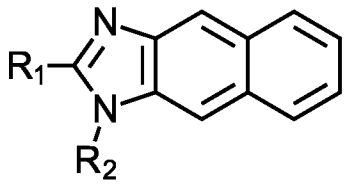

wherein R1 is selected from OH or H; and R2 is selected from a deoxyribose moiety of a polynucleotide, a ribose moiety of a polynucleotide, and a nucleic acid backbone mimic moiety.

Preferably, oligonucleotides are from about 6 to about 50 nucleotides in length. In still more preferred embodiments oligonucleotides are from about 12 to about 20 nucleotides in length.

Preferably, the oligonucleotides are complementary to a target polynucleotide such that the oligonucleotide is capable of forming a stable duplex with a target polynucleotide comprising O^6-alkyl guanine. It is understood in the art that a sequence need not be 100% complementary to that of its target sequence to form a duplex. The term complementarity is used herein to refer to a stretch of nucleic acids which can hybridise to another stretch of nucleic acids. It is thus not absolutely required that all the bases in the region of complementarity are capable of pairing with bases in the opposing strand. Mismatches may to some extent be allowed, if under the circumstances, the stretch of nucleotides is capable of hybridising to the complementary part. In some embodiments, a complementary part comprises at least 3, 4, 5, or 6 consecutive nucleotides complementary to the target polynucleotide.

In addition to comprising the base-modified-nucleoside analogs disclosed herein, the oligonucleotides may comprise additional nucleoside analogs containing natural and/or non-natural modifications and/or substitutions as disclosed herein, including stabilizing modifications/substitutions and purification or detection labels. The additional nucleoside analogs may contain synthetic and natural bases such as 5-methylcytosine (5-Me-C), 5-hydroxymethyl cytosine, xanthine, hypoxanthine, 2-

aminoadenine, 6-methyl and other alkyl derivatives of adenine and guanine, 2-propyl and other alkyl derivatives of adenine and guanine, 2-thiouracil, 2-thiothymine and 2-thiocytosine, 5-halouracil and cytosine, 5-propynyl uracil and cytosine and other alkynyl derivatives of pyrimidine bases.

The oligonucleotide may contain a backbone of ribose moieties, deoxyribose moieties, or nucleic acid backbone mimic moieties. The moieties may be connected by linkers well-known in the art such phosphodiester bonds, peptide bonds, and phosphorothioate linkages.

The preparation of oligonucleotides is well-known to a skilled person any includes the phosphodiester method disclosed in Brown E. L. et al (1979) *Methods Enzymol.,* 68: 109-151, the phosphotriester method described in Narang S. A. et al (1979) *Methods Enzymol.,* 68: 90-98, the diethylphosphoramidate method disclosed in Beaucage S. L., Caruthers M. H. (1981) *Tetrahedron Lett.,* 22: 1859-1862, as well as the use of either phosphoramidite chemistry or H-phosphonate chemistry. Other methods include those described in U.S. Pat. Nos. 4,659,774, 4,816,571, 5,141,813, 5,264,566, 4,959,463, 5,428,148, 5,554,744, 5,574,146, 5,602,244.

The compounds of the disclosure may be linked directly or indirectly to labels which aid in detection or purification. Suitable labels include, enzymes such as alkaline phosphatase and horseradish peroxidase, fluorescent proteins (e.g., GFP), bioluminescent proteins (e.g. aequorin), dyes, fluorescers (e.g., FRET probes), chemiluminescers radioactive groups. The detection of target duplexes may be performed using any number of methods known to a skilled person including fluorescence, chemiluminescence, bioluminescence, surface plasmon resonance, surface acoustic waves, mass spectrometry, infrared spectroscopy, Raman spectroscopy, atomic force microscopy, scanning tunneling microscopy, electrochemical detection methods, nuclear magnetic resonance, quantum dots, and the like.

The compounds of the disclosure may be immobilized to a solid substrate. The term "solid substrate" refers to any material that provides a solid structure with which an

oligonucleotide or nucleoside can be attached. Such materials include silicon, plastic, metal (e.g. gold electrode), glass, polymers, ceramic surfaces, and the like. A solid substrate may be of a rigid or non-rigid nature like gels, rubbers, polymers, etc. and it may be any type of shape including spherical shapes like beads and particles. Compounds of the disclosure are immobilized to a solid substrate directly or indirectly, preferably through a covalent bond using a spacer molecule or linker group. The immobilization of the compounds of the disclosure on a solid substrate can aid in isolating target duplexes and for immobilizing bound target nucleic acid. In some embodiments, the solid substrates act aid in the detection of duplex formation (e.g., quantum dots (fluorescence), gold nanoparticles (aggregation), gold electrode (conductivity), cantilever (surface tension)).

The solid substrates may also be useful to provide oligonucleotides in an arrayed format. Preferably, a solid surface (e.g., DNA chip/microarray) is provided comprising an array of oligonucleotides comprising ExBIM or Exbenzi.

Preferably, the solid substrate is a particle such as latex or carbon particle. Preferably the particle is a nanoparticle such as metal (preferably gold or silver), semiconductor, insulator, magnetic, or a quantum dot, more preferably the particle is a gold nanoparticle. The size of the nanoparticles is preferably from about 5 nm to about 150 nm (mean diameter), more preferably from about 5 to about 50 nm, most preferably from about 10 to about 30 nm. Methods of making such nanoparticles are well-known in the art. Either the nanoparticles, the oligonucleotides or both are functionalized by methods known in the art in order to attach the oligonucleotides to the nanoparticles. In exemplary embodiments, oligonucleotides are terminated with a 5′ thionucleoside or a 3′ thionucleoside for attaching to solid surfaces.

Preferred aspects of the disclosure provide for the use of the compounds of the disclosure for detecting the presence of O^6-alkyl guanine, preferably for detecting the presence of O^6-alkyl guanine in a target polynucleotide. Preferably, the disclosure provides for the use of an oligonucleotide comprising at least one base-modified-nucleotide analog as disclosed herein for detecting the presence of O^6-alkyl guanine in a target polynucleotide, wherein said oligonucleotide is complementary to said

polynucleotide such that said target polynucleotide and said oligonucleotide form a target duplex.

The detection of the presence of O^6-alkyl guanine can be determined by measuring the binding of the base-modified-nucleoside analogs to O^6-alkyl guanine or by measuring the formation of a duplex between the oligonucleotide and the O^6-alkyl guanine in a target polynucleotide("target duplex").

Binding and duplex formation can be measured by various assays well-known in the art. The stability of duplex formation can be determined by analysing duplex formation under various conditions. The formation of a duplex formed by the target polynucleotide and the oligonucleotide (i.e., the target duplex) can be compared to the formation of a duplex formed by the oligonucleotide and a control nucleic acid sequence. The control nucleic acid sequence preferably has the same nucleic acid sequence as the target sequence but lacks O^6-alkyl guanine. An increase in the amount of duplex formation of the target duplex over the control duplex indicates the presence of O^6-alkyl guanine in the target polynucleotide.

Accordingly, methods are provided for detecting the presence of O^6-alkyl guanine in a target polynucleotide comprising a) contacting a target polynucleotide with an oligonucleotide comprising Exbenzi or ExBIM, wherein said oligonucleotide is complementary to said target polynucleotide such that said target sequence and said oligonucleotide form a duplex and b) measuring the formation or stability of said duplex.

Preferably, the method further comprises c) comparing the formation of the target duplex to the formation or stability of a duplex formed by said oligonucleotide with a control nucleic acid sequence not having O^6-alkyl guanine, wherein an increased formation or stability of the target duplex over the control duplex indicates the presence of O^6-alkyl guanine in said nucleic acid sequence.

In preferred embodiments, the methods comprise a) contacting a target polynucleotide with a first oligonucleotide that is complementary to said target polynucleotide and a

second oligonucleotide that is complementary to said target polynucleotide such that said target polynucleotide can simultaneously hybridize to both the first and second oligonucleotides forming a duplex; wherein the first oligonucleotide is an oligonucleotide comprising Exbenzi or ExBIM and b) measuring the formation or stability of said duplex. In these embodiments, the resulting close proximity of the two oligonucleotides may be used to measure the formation or stability of said duplex.

Preferably, the method further comprises c) comparing the formation of the target duplex to the formation or stability of a duplex formed by said oligonucleotides with a control nucleic acid sequence not having O^6-alkyl guanine, wherein increased formation or stability of the target duplex over the control duplex indicates the presence of O^6-alkyl guanine in said nucleic acid sequence.

In an alternative embodiment, the second oligonucleotide is complementary to said first oligonucleotide such that said second oligonucleotide competes with the target polynucleotide for binding to the first oligonucleotide. In this embodiment, the first oligonucleotide comprises Exbenzi or ExBIM and the second oligonucleotide does not comprise O^6-alkyl guanine. Since Exbenzi and ExBIM form more stable bonds with O^6-alkyl guanine over guanine, the first oligonucleotide (comprising Exbenzi or ExBIM) will form a more stable duplex with a target polynucleotide which contains O^6-alkyl guanine as compared to the second oligonucleotide (not containing O^6-alkyl guanine). Preferably, the second oligonucleotide in these embodiments has either the same sequence as the target polynucleotide or differs only by the presence of guanine instead of O^6-alkyl guanine.

The contacting of the oligonucleotides with the target polynucleotide takes place under conditions effective for hybridization of the ExBIM/Exbenzi oligonucleotide with the target sequence of the nucleic acid. These hybridization conditions are well known in the art and can readily be optimized for the particular system and target polynucleotide employed. It is clear to a skilled person that these conditions can be optimized such that the target duplex is able to form but the conditions are too stringent for control duplex formation. This can be achieved, for example, by increasing temperature and altering salt concentrations. In such an embodiment,

control duplex formation does not occur (or occurs at a much reduced rate as compared to target duplex formation).

Methods to measure formation and stability of nucleic acid duplexes are well-known to the skilled person. In some embodiments, the duplex is heated in solution until the strands of the duplex separate. The stability of a duplex is expressed by the temperature at which one-half the base pairs have dissociated, commonly known as the "melting temperature" or Tm. In practice, this is usually measured by monitoring the ultraviolet absorbance of a solution of nucleic acid while the temperature is increased and denoting the Tm as the temperature at half the maximal absorbance at 260 nm.

Methods to measure formation and stability can also be performed using labelled nucleoside analogs or oligonucleotides. In further embodiments, the first oligonucleotide is provided with a first detectable label and the second oligonucleotides is provided with a second detectable label such that the close physical proximity of the first and second labels resulting from duplex formation leads to a measurable parameter. In some embodiments the first and second detectable label are the same, in some embodiments they are different.

Exemplary labels include hybridization probes such as FRET probes. FRET probe refers to a fluorescent oligonucleotide which is used for detection of a target polynucleotide wherein detection is based on the FRET effect. The FRET probe commonly contains two chromophores, an acceptor chromophore and a reporter fluorophore. The acceptor chromophore is usually a non-fluorescent dye chosen to quench fluorescence of the reporting fluorophore. Formation of target duplexes leads to a change in fluorescent properties. (see Didenko, Biotechniques. Nov 2001; 31(5): 1106–1121 for a review of FRET based hybridization probes).

In some embodiments, a hairpin oligonucleotide complementary to the target polynucleotide comprises both acceptor and reporter chromophores and Exbenzi or ExBIM. Binding of the oligonucleotide to the target polynucleotide results in a change in fluorescent properties.

In other embodiments, a first oligonucleotide having an acceptor chromophore is provided together with a second oligonucleotide having a reporter chromophore, such that both oligonucleotides can simultaneously bind the target nucleic acid, wherein at least one of the oligonucleotides comprises Exbenzi or ExBIM. Formation of a target duplex comprising both oligonucleotides and the target polynucleotide results in a change in fluorescent properties.

In preferred embodiments, competitive hybridization is performed wherein a first oligonucleotide being complementary to the target polynucleotide and having an acceptor chromophore and comprising Exbenzi or ExBIM is provided together with a second oligonucleotide being complementary to the first oligonucleotide and having a reporter chromophore, such that the target polynucleotide and the second oligonucleotide compete for binding to the first oligonucleotide. If the target nucleotide contains O^6-alkyl guanine it will bind more stably to the first oligonucleotide than the second oligonucleotide not containing O^6-alkyl guanine.

In some embodiments, the oligonucleotides are attached to quantum dots. The term "quantum dot" (QD) refers to semiconductor or insulator nanoparticles that may comprise a dopant. The wavelength of the light emitted (e.g., color) by the QD can be selected according to the physical properties of the nanoparticles, such as size, material, and the dopant. QD assays are known to a skilled person and are also described in US20130029333.

In some embodiments, an oligonucleotide comprising ExBIM or Exbenzi is attached to a QD. In some embodiments of the methods, the first oligonucleotide is attached to a first quantum dot and the second oligonucleotide is attached to a second quantum dot. Preferably, the quantum dots are selected such that each emits at a different wavelength under the same excitation source.

In an exemplary embodiment, the first oligonucleotide comprising ExBIM or Exbenzi is attached to QD565 and the second oligonucleotide is attached to QD655. The

oligonucleotides are contacted with a nucleic acid sample. Target duplexes are detected by measuring fluorescence.

In preferred embodiments, oligonucleotides are attached to nanoparticles and the aggregation of the nanoparticles is used as a readout for target duplex formation. Preferably said nanoparticles are gold nanoparticles (AuNP). Aggregation of said particles can be detected by color change, fluorescence, radioactivity, quartz crystal microbalance, Raman spectroscopy, light scattering, and electrical signals. AuNPs are easily conjugated with biomolecules and retain the biochemical activity of the tagged biomolecules. Methods for preparing oligonucleotide bound gold particles are disclosed in the examples and are also described in WO 2008042156.

The examples describe an exemplary embodiment in which AuNPs are conjugated to oligonucleotides designed to hybridize with DNA bearing an O^6-meG adduct. Selective hybridization is enabled by incorporating into the oligonucleotide probe the novel nucleoside ExBIM. AuNP probes were constructed such that ExBIM is positioned to pair opposite the target DNA adduct within a defined DNA sequence. DNA hybridization results in self-assembly and aggregation of AuNPs.

The oligonucleotides comprising ExBIM or Exbenzi are also useful for enriching or isolating a target nucleic acid. Isolating a target polynucleotide refers to increasing the number or concentration of said target or reducing the amount of non-target polynucleotide from a sample.

Accordingly, a method is provided for isolating an O^6-alkyl guanine containing target nucleic acid, said method comprising a) contacting a nucleic acid containing sample with an oligonucleotide comprising ExBIM or Exbenzi, wherein said oligonucleotide is complementary to said target polynucleotide such that said target sequence and said oligonucleotide form a target duplex and b) isolating said target duplex. Preferably the oligonucleotide is coupled to a purification label or a solid substrate and the target duplex is isolated via the label or substrate. Suitable solid substrates have been disclosed herein. For example, the substrate may be a magnetic bead and target duplexes are separated from the sample with a magnetic field. Purification labels

(e.g., biotin) are well-known to the skilled person and are also further described herein. Example 3 provides an exemplary embodiment of a method for isolating a O^6-alkyl guanine containing target nucleic acid.

It is understood that methods for isolating an O^6-alkyl guanine containing target polynucleotide can be used in conjunction with methods for detecting the presence of O^6-alkyl guanine in a target nucleic acid. In an exemplary embodiment, a first oligonucleotide comprising ExBIM or Exbenzi is attached to a magnetic bead. The nucleic acid containing sample is contacted with said first oligonucleotide and a magnetic field is applied to separate the target duplexes from the rest of the sample. The target duplex is heated to denature the duplex. The first oligonucleotide is removed by applying a magnetic field. The isolated target polynucleotide can then be detected by the methods disclosed herein, e.g., using FRET hybridization probe or gold particle aggregation. Combining an isolation step with a detection step can increase the sensitivity and/or reduce the background of the methods.

Definitions

As used herein, "to comprise" and its conjugations is used in its non-limiting sense to mean that items following the word are included, but items not specifically mentioned are not excluded. In addition the verb “to consist” may be replaced by “to consist essentially of” meaning that a compound or adjunct compound as defined herein may comprise additional component(s) than the ones specifically identified, said additional component(s) not altering the unique characteristic of the invention.

The articles “a” and “an” are used herein to refer to one or to more than one (i.e., to at least one) of the grammatical object of the article. By way of example, “an element” means one element or more than one element.

The word “approximately” or “about” when used in association with a numerical value (approximately 10, about 10) preferably means that the value may be the given value of 10 more or less 1% of the value.

All patent and literature references cited in the present specification are hereby incorporated by reference in their entirety.

The invention is further explained in the following examples. These examples do not limit the scope of the invention, but merely serve to clarify the invention.

EXAMPLES

Example 1:

Phosphoramidite and oligonucleotide synthesis. Phosphoramidites of Exbenzi and ExBIM nucleosides were synthesized (Scheme 1; Figure4) for their site-specific incorporation into oligonucleotides. Exbenzi nucleobase **7** was prepared in a solvent-free reaction by heating 2,3-diaminonaphtalene and urea in a microwave,(Kidwai et al., 2005) and ExBIM nucleobase **8** was prepared by heating 2,3-diaminonapthalene in formic acid.(Herbert et al., 1987; Sachs, 1909) The nucleobases were glycosylated by nucleophilic displacement of chloride from 1-(α)-chloro-3,5-di-*O*-*p*-toluoyl-2-deoxyribose (**9**) to yield tolouylated nucleosides, which were deprotected by trans-esterification with NaOMe to yield free nucleosides **5** and **6**. Protection of the 3'-OH of **5** and **6** was initially attempted using DMTCl, but very low yields of product were obtained. Thus, DMT groups were installed with the more reactive reagent DMT·BF_4 to obtain **10** and **11**.(Bleasdale et al., 1990; Hansen et al., 2011; Lakshman and Zajc, 1996) Finally, phosphoramidites **13** and **14** were formed by alkylating the 5'-OH of **10** and **11** with chlorinated phosphotidylating reagent **12**.(Gong and Sturla, 2007) Per, Peri, BIM, and Benzi nucleosides and phosphoramidites were synthesized as reported elsewhere.(Gahlon and Sturla, 2013a; Gong and Sturla, 2007)

Oligonucleotides with sequences 5'-CCGXTATACCGACAA-3' (X = ExBenzi or ExBIM) were prepared by solid-phase DNA synthesis; this sequence was selected to allow direct comparison with published data examining related interactions.(Gahlon and Sturla, 2013a; Gong and Sturla, 2007) For dangling-end studies, the sequence 5'-XCGCGCG-3', which has previously been used to characterize π-stacking of both natural nucleosides and nucleoside analogs,(Gao et al., 2004; Guckian et al., 2000; Lai and Kool, 2004; Lee and Kool, 2005; Liu et al., 2005; Lu et al., 2004; Rosemeyer and Seela, 2002) was selected. Incorporation of nucleoside analog phosphoramidites was typically half as efficient as that of the natural nucleotide phosphoramidites (as indicated by UV absorbance trityl cation monitoring), and the major side-products

were oligonucleotides truncated immediately prior to Exbenzi or ExBIM incorporation.

DNA duplex stability. The melting of DNA duplexes containing nucleoside analogs of Per, Exbenzi, and ExBIM paired opposite G, O^6-Me-G or O^6-Bn-G was monitored by UV spectroscopy. The thermodynamic stabilities of the duplexes (i.e., the free energies of melting, ΔG) were calculated both by analyzing the shape of the melting curve to obtain $\Delta G_{CF}°$ and, for the purpose of comparison with previously reported nucleoside analogs,(Gahlon and Sturla, 2013b) by evaluating the dependence of the melting transition temperature on the duplex concentration to obtain $\Delta G_{TT}°$ (Table 1). While $\Delta G_{TT}°$ values are more commonly reported since they are less time-consuming to derive, $\Delta G_{CF}°$ values are more precise, and because a $\Delta G_{CF}°$ can be derived from each individual experiment, the data are more amenable to statistical analysis (Figure 2). Free energies derived from the dependence of duplex melting temperatures as opposed to transition temperatures were also determined ($\Delta G_{TM}°$), but for simplicity only $\Delta G_{TT}°$ and $\Delta G_{CF}°$ are discussed below.

TABLE 1. Free energies of probe:target melting.[a]

P	X	*n* [b]	$\Delta G_{TT}°$ [c]	$\Delta\Delta G_{TT}°$[d]	$\Delta G_{CF}°$ [e]	$\Delta\Delta G_{CF}°$
Per	**G**	12	-16.6 ± 5.6		-15.6 ± 0.1	
	O⁶MeG	7	-18.2 ± 11.8	-1.6	-16.6 ± 0.4	-1.0
	O⁶BnG	9	-17.9 ± 12.0	-1.3	-16.6 ± 0.4	-1.0
	THF	10	-16.2 ± 5.6	0.4	-15.5 ± 0.2	0.1
Exbenzi	**G**	18	-15.1 ± 4.5		-15.5 ± 0.4	
	O⁶MeG	29	-18.1 ± 10.5	-3.0	-17.2 ± 0.6	-1.7
	O⁶BnG	12	-17.0 ± 6.5	-1.9	-17.8 ± 0.4	-2.2
	THF	18	-15.7 ± 4.7	-0.6	-16.3 ± 0.3	-0.8
ExBIM	**G**	17	-15.4 ± 3.6		-16.2 ± 0.3	
	O⁶MeG	18	-17.9 ± 5.9	-2.5	-16.7 ± 0.3	-0.5
	O⁶BnG	18	-16.4 ± 6.7	-1.0	-16.9 ± 0.3	-0.7
	THF	18	-16.5 ± 5.9	-1.1	-17.0 ± 0.4	-0.8

[a]Duplex = 5'-TTGTCGGTATAXCGG-3' complementary to 3'-AACAGCCATATPGCC-5', in which X = nucleosides of G, *O*⁶-Me-G, or *O*⁶-Bn-G and P = nucleoside analog. All thermodynamic parameters (with standard errors) are reported in kcal/mol. Standard errors for values derived from plots of $1/T_t$ vs ln C_T and $1/T_m$ vs ln C_T are propagated from standard errors of the slopes and intercepts, as obtained from the LINEST function in Excel. $\Delta G°$ values were calculated prior to rounding $\Delta S°$ and ΔH (Table 1) to the nearest decimal place. [b]Number of separately prepared samples. [c]Values derived from plots of $1/T_t$ vs ln C_T. [d]$\Delta\Delta G° = \Delta G°$(**P**:adduct) - $\Delta G°$(**P**:**G**). [e]Values derived using the curve-fit method.

The extent to which a nucleoside analog discriminates between *O*⁶-alkyl-G and G is reflected in the difference in stabilities of DNA duplexes containing analog:adduct pairs and analog:G pairs ($\Delta\Delta G° = \Delta G°$(analog:adduct) - $\Delta G°$(analog:G)). In our study, we found that the relative abilities of nucleoside analogs to discriminate between G and *O*⁶-alkyl-G were dependent on the model used to calculate $\Delta G°$. On the basis of $\Delta G_{CF}°$ values (Table 1, Figure 2), Exbenzi was the best able to distinguish between G vs *O*⁶-Me-G and *O*⁶-Bn-G ($\Delta\Delta G_{CF}°$ = -1.6 and -2.2 kcal/mol, respectively), followed by Per ($\Delta\Delta G_{CF}°$ = -1.0 and -1.0 kcal/mol) and then ExBIM ($\Delta\Delta G_{CF}°$ = -0.5 and -0.7 kcal/mol). Considering $\Delta G_{TT}°$ values instead (Table 1), Exbenzi again discriminated best between G vs *O*⁶-Me-G and *O*⁶-Bn-G ($\Delta\Delta G_{TT}°$ = -3.0 and -1.9 kcal/mol, respectively), while Per showed better discrimination than ExBIM opposite *O*⁶-Bn-G

($\Delta\Delta G_{TT}°$ = -1.3 and -1.0 kcal/mol, respectively) but not opposite O^6-Me-G ($\Delta\Delta G_{TT}°$ = -1.6 and -2.5 kcal/mol, respectively). For comparison, the naphthalene-derived Peri showed moderate preference for O^6-Me-G than G ($\Delta\Delta G_{TT}°$ = -2.2 kcal/mol) and weaker preference for O^6-Bn-G than G ($\Delta\Delta G_{TT}°$ = -1.2 kcal/mol), while the smaller nucleosides, Benzi and BIM, discriminated modestly between G vs O^6-Me-G ($\Delta\Delta G_{TT}°$ = -1.7 and -1.6 kcal/mol, respectively) and very weakly between O^6-Bn-G vs G ($\Delta\Delta G_{TT}°$ = -0.5 and -0.6 kcal/mol, respectively) (Table 2).(Gahlon and Sturla, 2013b)

Table 2: Free energies of probe:target melting.[a] probe:target melting.[a]

P	X	$\Delta G_{TT}°$ [c]	$\Delta\Delta G_{TT}°$ [d]
Peri	**G**	-16.2	
	O⁶MeG	-18.4	-2.2
	O⁶BnG	-17.4	-1.2
	THF	-15.9	0.3
Benzi	**G**	-15.2	
	O⁶MeG	-16.9	-1.7
	O⁶BnG	-15.7	-0.5
	THF	-14.0	1.2
BIM	**G**	-14.6	
	O⁶MeG	-16.2	-1.6
	O⁶BnG	-15.2	-0.6
	THF	-13.9	0.7

[a]Duplex = 5'-TTGTCGGTATAXCGG-3' complementary to 3'-AACAGCCATATPGCC-5', in which X = nucleosides of G, O^6-Me-G, or O^6-Bn-G and P = nucleoside analog. All thermodynamic parameters (with standard errors) are reported in kcal/mol. [c]Values derived from plots of $1/T_t$ vs ln C_T. [d]$\Delta\Delta G° = \Delta G°$(**P**:adduct) - $\Delta G°$(**P**:**G**). [e]Values derived using the curve-fit method. n.r. = not reported. n.d. = not determined.

The ability of each nucleoside analog to stabilize a different lesion, the model abasic site THF, was also tested. Abasic sites are one of the most ubiquitous forms of DNA damage, occuring at a background physiological rate of about 10,000 times per human genome per day.(Lindahl, 1993) Thus, evaluating the stability of analog:THF pairs is important for rating the specificity of the analogs toward their intended O^6-alkyl-G targets. According to $\Delta G_{CF}°$ values, Exbenzi is the only analog that shows statistically significant differentiation between G, O^6-Me-G, O^6-Bn-G, and THF ($\Delta G_{CF}°$ = -15.5, -

17.2, -17.8, and -16.3 kcal/mol, respectively) (Table 1, Figure 2). Although Per formed more stable pairs opposite O^6-Me-G and O^6-Bn-G than opposite THF ($\Delta G_{CF}°$ = -16.6, -16.6, and -15.5 kcal/mol, respectively), it did not distinguish between G and THF ($\Delta\Delta G_{CF}°$ = 0.1 kcal/mol). Meanwhile, ExBIM showed no distinction between O^6-Me-G, O^6-Bn-G, and THF ($\Delta G_{CF}°$ = -16.7, -16.9, and -17.0 kcal/mol, respectively). Similar trends are observed when $\Delta G_{TT}°$ values are considered, with the exception that Per seemed to show a slightly greater preference for THF than for G ($\Delta G_{TT}°$ = -16.2 and -16.6 kcal/mol, respectively) and that ExBIM appeared to form a stronger pair opposite O^6-Me-G ($\Delta G_{TT}°$ = -17.9 kcal/mol) than opposite O^6-Bn-G and THF ($\Delta G_{TT}°$ = -16.4 and -16.5 kcal/mol, respectively) (Table 2).

A comparison between the relative stabilities of Exbenzi and ExBIM vs Benzi and BIM opposite abasic sites reveals the potential impact of large nucleobase surface area and elongated shape on π-stacking within the DNA duplex. Exbenzi and ExBIM imparted greater duplex stability when placed opposite THF ($\Delta G_{TT}°$ = -15.7 and -16.5 kcal/mol, respectively) than did Benzi and BIM ($\Delta G_{TT}°$ = -14.0 and -13.9 kcal/mol, respectively)(Gahlon and Sturla, 2013b) (Tables 1 and 2). Presumably, the elongated nucleobases of Exbenzi and ExBIM are better than those of Benzi and BIM at filling the gap of the abasic site and π-stacking with neighboring nucleobases.

Evaluating π-stacking. To assess the π-stacking of nucleoside analogs, their ability to stabilize the termini of short DNA duplexes was evaluated. Such experiments have been used to systematically explore the impact of dipole moment, polarizability, and hydrophobicity on the ability of natural and non-natural bases to contribute to DNA stabilization apart from hydrogen bonding or other interactions with complementary partners.(Gao et al., 2004; Guckian et al., 2000; Isaksson and Chattopadhyaya, 2005; Lai and Kool, 2004; Lee and Kool, 2005; Liu et al., 2005; Lu et al., 2004; Morales-Rojas and Kool, 2002; Nakano et al., 2011; Rosemeyer and Seela, 2002) In these experiments, the thermal stabilities (ΔG_{CF}^{37}) of duplexes containing dangling residues on the 5'-end of a self-complementary oligonucleotide (5'-XCGCGCG-3') were determined (Table 3). This sequence was selected since the G-C content precludes minor groove binding of the dangling residue(Guckian et al., 2000) and is known to form a B-DNA duplex structure at NaCl concentrations below 2.5 M.[21,](Gao et al., 2004; Guckian et al., 2000; Lai and Kool, 2004; Lee and Kool, 2005; Liu et al., 2005; Lu et al., 2004; Rosemeyer and Seela, 2002) Previous studies indicated that the dipole

moment or hydrophobicity (as reflected in log P values and retention time in reverse-phase chromatography) of nucleoside analogs did not correlate to dangling-end stabilization.[29,38] Rather, nucleobase polarizability and surface area (which influences both polarizability and shielding of the duplex from solvent) robustly correlated to dangling nucleoside stabilization.(Guckian et al., 2000; Rosemeyer and Seela, 2002)

TABLE 3. Dangling-end stabilization.[a]

P	S.A. (Å^2) [b]	*n* [c]	ΔG_{CF}^{37}	Lit. ΔG^{37}
–	n.d.	11	-8.9 ± 0.1	-8.1 ± 0.1 [d]
Per	n.d.	8	-10.5 ± 0.1	n.d.
Peri	n.d.	5	-11.7 ± 0.1	n.d.
Benzi	n.d.	6	-10.9 ± 0.2	n.d.
BIM	n.d.	5	-10.2 ± 0.1	n.d.
Exbenzi	n.d.	7	-11.3 ± 0.2	n.d.
ExBIM	n.d.	7	-11.8 ± 0.3	n.d.
A	142	4	-10.5 ± 0.1	-10.0 ± 0.4 [d]
G	154	4	-10.5 ± 0.1	-9.9 ± 0.3 [d]
C	127	7	-9.6 ± 0.1	-8.9 ± 0.1 [d]
T	142	5	-9.9 ± 0.1	-9.2 ± 0.9 [d]
Benzene	110	n.r.	n.d.	-9.4 ± 0.7 [d]
Naphthalene	158	n.r.	n.d.	-10.9 ± 0.1 [d]
Pyrene	217	n.r.	n.d.	-11.3 ± 0.3 [d]
xA	n.d.	n.r.	n.d.	-12.1 ± 0.2 [e]
xC	n.d.	n.r.	n.d.	-10.1 ± 0.3 [f]
xT	n.d.	n.r.	n.d.	-11.1 ± 0.3 [e]

[a] Duplex = 5'-PCGCGCG-3' : 3'-GCGCGCP-5', in which P = designated nucleoside. All free energies are reported in kcal/mol. Errors indicate standard error. [b] Half of the calculated surface area of the free nucleobase (ref 29). [c] Number of separately prepared samples. [d] Data derived from curve fits (ref. 29). [e] Data derived from curve fits (ref. 34). [f] Data averaged from concentration dependent and curve fit methods (ref. 32). n.d. = not determined. n.r. = not reported.

In this study, we also observed that as the surface area of the dangling-end nucleoside increased, the more it stabilized the duplex. Among the nucleoside analogs, Exbenzi, ExBIM, and Peri stabilized the duplex the most (ΔG_{CF}^{37} = -11.3, -11.8, -11.7 kcal/mol, respectively), while Per and Benzi showed moderate stabilization (ΔG^{37} = -10.5 and -

10.9 kcal/mol, respectively) and BIM, with the smallest surface area, stabilized the duplex the least (ΔG_{CF}^{37} = -10.2 kcal/mol). Notably Benzi and BIM, which have similar size and shape as purine nucleosides, stabilized the duplex to a similar extent as did A and G (Exp. ΔG_{CF}^{37} = -10.5 kcal/mol each, Lit. ΔG^{37} = -10.0 and -9.9 kcal/mol, respectively).(Guckian et al., 2000) Duplexes containing dangling pyrimidines were the least stable (Exp. ΔG_{CF}^{37} = -9.6 and -9.9 kcal/mol, Lit. ΔG^{37} = -8.9, and -9.2 kcal/mol for C and T, respectively).(Guckian et al., 2000) On the basis of their strong dangling-end stabilization, we presume that Exbenzi, ExBIM, and Peri nucleosides adopt conformations that allow their nucleobases bases to shield the hydrogen bonds of the terminal G:C base pairs from water molecules that would disrupt the hydrogen bonds.(Isaksson and Chattopadhyaya, 2005).

Our results are consistent with previous reports that larger nucleobases generally π-stack more strongly than smaller nucleobases since they have more surface area of overlap with neighboring bases. This effect is specifically demonstrated in studies evaluating the stacking capabilities of benzene, naphthalene, and pyrene nucleosides (Lit. ΔG^{37} = -9.4, -10.9, and -11.3 kcal/mol, respectively)(Guckian et al., 1996; Guckian et al., 2000) or comparing A, C, and T to their elongated counterparts xA, xC, and xT (Lit. ΔG^{37} = -12.1, -10.1, and -11.1 kcal/mol, respectively).(Gao et al., 2004; Lee and Kool, 2005; Liu et al., 2005) Bigger nucleobases do not necessarily have better overlap with neighboring base pairs due to their shape or glycosidic orientation, as Kool's study comparing the pyrene nucleoside with a larger porphyrin nucleoside demonstrated.(Morales-Rojas and Kool, 2002) Thus, although the surface area of Per is similar to that of Peri, the carbonyl group present on Per may induce a conformation that is not favorable for dangling-end π-stacking, causing it's relatively low dangling-end stabilization.

Quantum yields of nucleoside analogs. A quantitative measure of the fluorescence of a compound that allows comparison to other fluorophores is the quantum yield Φ_f. Quantum yield is defined by the ratio of amount of photons absorbed to the amount of photons emitted through fluorescence.(Sinkeldam et al., 2010) Fluorescence quantum yields of nucleoside analogs were determined relative to standards tryptophan (water, pH 7) and 2-aminopyridine (0.05 M H_2SO_4) using the comparative method.(Williams, 1983) We found our quantum yields for tryptophan ($\Phi_{f,\,measured}$ = 0.10) and 2-

aminopyridine ($\Phi_{f, measured}$ = 0.71) to be in reasonable agreement with those previously reported ($\Phi_{f, lit}$ = 0.12(Chen, 1967)and $\Phi_{f, lit}$ = 0.60,(Rusakowicz, 1968) respectively). The following quantum yields of nucleoside analogs were determined (Table 4): BIM (Φ_f = 0.82) > Exbenzi (Φ_f = 0.69) > ExBIM (Φ_f = 0.44) > Benzi (Φ_f = 0.35). Per and Peri nucleosides were not measurably fluorescent (data not shown). The quantum yield of Benzi (Φ_f = 0.35) is very similar as previously reported for the nucleobase benzimidazolone (Φ_f = 0.34).(Lazar et al., 2003) All nucleoside analogs tested herein had emission maxima in the UV range (Figure S1, Table 4); those with a larger π-surface area (ExBIM and Exbenzi) emit fluorescence at a higher wavelength (364 nm and 338 nm, respectively) compared to smaller nucleosides BIM and Benzi (297 nm and 309 nm, respectively).

TABLE 4: Quantum yields (Φf) of nucleoside analogs. [a]

Compound (solvent)	Φf, measured [b]	λem, max
Tryptophan (water)	0.10	346 nm
2-Aminopyridine (0.05 M H_2SO_4)	0.71	358 nm
Benzi (10% DMSO)	0.35	309 nm
BIM (10% DMSO)	0.82	297 nm
Exbenzi (10% DMSO)	0.69	338 nm
ExBIM (10% DMSO)	0.44	364 nm

[a] Obtained relative to standards tryptophan and 2-aminopyridine. [b] Excitation wavelength 250 nm.

Fluorescence of DNA containing nucleoside analogs. When Exbenzi and ExBIM were incorporated into ssDNA, the emission maxima shifted to 384 nm and 350 nm, respectively and the emission intensity was much lower than that of free nucleosides at comparable concentration. For comparison, ssDNA comprised of natural nucleosides showed no detectable fluorescence Upon hybridization of the nucleoside analog-containing probe strands to complementary strands containing G, O^6-Me-G, or THF, the fluorescence was quenched relative to that of ssDNA (on the order of 20 fold for ExBIM and 10 fold for Exbenzi).

General. Anhydrous solvents were purified through an LC Technology Solutions solvent purification system, in which the solvent is passed through a column of

activated alumina before being dispensed under nitrogen, or were purchased from Sigma-Aldrich and used without further drying or purification. Diamines, nitrogen bases, and sodium hydride were purchased from Sigma-Aldrich and used without further purification. 1-(α)-Chloro-3,5-di-*O*-*p*-toluoyl-2-deoxy-D-ribose (**9**) was obtained from Berry & Associates, and 2-cyanoethoxy-*N*,*N*-diisopropylaminochlorophosphine (**12**) was obtained from Link Technologies and Sigma-Aldrich. 4,4'-Dimethoxyltrityl tetraflouroborate (DMT·BF_4) was prepared from 4,4'-dimethoxytrityl chloride (DMTCl) as described previously.(Hansen et al., 2011) The O^6-Bn-G phosphoramidite was synthesized beginning from 2',3',N^2-triacetyl-dG prepared as described.(Lee et al., 1995) O^6-Benzylation of 2',3',N^2-triacetyl-dG was carried out using Mitsunobu reaction conditions like those previously indicated, except that tetrahydrofuran was used as the solvent instead of dioxane.(Gillet and Schaerer, 2002; Lee et al., 1995) Following deacetylation of the 3' and 5' hydroxyl groups,(Mounetou et al., 1997) the 5' hydroxyl was protected with a 4,4'-dimethoxytrityl group and subsequently the protected nucleoside was converted to the phosphoramidite using conditions previously described.(Gong and Sturla, 2007)

^{1}H NMR spectra were acquired at 400 MHz and ^{13}C NMR at 100 MHz on a Bruker NMR spectrometer. Chemical shifts are reported relative to the non-deuterated solvent signals (3.31 and 49.05 ppm in MeOH-d_4, 2.50 and 39.43 in DMSO-d_6, and 2.05 and 30.83 in acetone-d_6 for ^{1}H and ^{13}C NMR spectra, respectively). Flash chromatography (silica gel 60Å 200-400 mesh) was used for product purification. Normal phase thin-layer chromatography (TLC; plates obtained from Silicycle) was used for reaction monitoring and the spots were visualized under UV light (254 nm). High-resolution ESI-MS (HRMS) was performed on a Thermo Scientific Exactive mass spectrometer. UV absorptions were measured at 260 nm using a Cary 100 UV-Vis spectrophotometer equipped with a Peltier thermal programmer.

1*H*-naphtho[2,3-*d*]imidazol-2(3*H*)-one (7). According to a previously described method,(Kidwai et al., 2005) 2,3-diaminonapthalene (430 mg, 2.77 mmol) and urea (218 mg, 3.63 mmol) were added to a 100 mL Erlenmeyer flask. The flask was heated for 15 min in a 700W kitchen microwave, with stopping every 5 minutes to break up and stir the chunky bronze-colored reaction mixture. The product was suspended in 5% aqueous HCl, and the precipitate was filtered off and washed twice more with 5% HCl and twice with water. The gold-colored solid was then dried under vacuum to

yield product (84% yield). ^{1}H NMR (DMSO-d_6): 10.797 (s, 1.9 H), 7.80 (m, 2H), 7.28 (m, 4H). ^{13}C NMR (DMSO-d_6): 156.14, 131.00, 129.16, 123.22, 103.55. ESI-MS: M+H$^+$ calc'd 185.0709, found 185.0711.

1'-β-[1-naphtho[2,3-*d*]imidazol-2(3*H*)-one)]-2'-deoxy-D-ribofuranose (**5**). The synthesis of the Exbenzi nucleoside was adapted from that previously described for the preparation of the Per nucleoside.(Gong and Sturla, 2007) Exbenzi nucleobase **7** (1.103 g, 5.50 mmol) and anhydrous THF (50 mL) were added to a flame-dried 100 mL flask and flushed with nitrogen for several minutes. To the mixture, NaH (60% in mineral oil, 333 mg, 8.25 mmol) was added portion-wise over 2 minutes. The flask was again flushed with N_2 for several minutes, and the dark brown suspension with chunky gold precipitate was allowed to stir for 0.5 h. Then, a suspension of 1-(α)-Chloro-3,5-di-*O*-*p*-toluoyl-2-deoxy-D-ribose (**9**) (2.14 g, 5.50 mmol) in anhydrous THF (10 mL) was added dropwise to the stirring suspension of **7** over 0.5 h. After another 1.5 h stirring, during which TLC indicated no further conversion, the reaction was quenched with H_2O (15 mL) and concentrated to dryness with rotatory evaporation. To remove the remaining Exbenzi from the reaction mixture, the solid was suspended in 1:1 DCM/MeOH (50 mL). The suspension was centrifuged, the supernatant removed, and the precipitated Exbenzi re-suspended and centrifuged again out of 20 mL MeOH. The supernatants were pooled and concentrated, then chromatographed using a 0-10% MeOH in DCM gradient. Bis-toluoyl protected nucleoside (44 mg, 0.082 mmol), mono-toluoyl protected nucleoside (120 mg, 0.306 mmol), and fully deprotected nucleoside (65 mg, 0.218 mmol) were obtained, for a total of 11% conversion of Exbenzi.

The bis- and mono-toluoyl protected nucleosides (44 mg, 0.082 mmol and 120 mg, 0.306 mmol, respectively) were pooled and dissolved in THF (9 mL). NaH (60% in mineral oil, 29 mg, 0.73 mmol) was added, then MeOH (1 mL) was added dropwise. After 2 min, the mixture was dried by rotatory evaporation and chromatographed using a 3-10% MeOH in DCM gradient. Fully deprotected nucleoside was pooled with that obtained from the first step, for a total of 97 mg (0.32 mmol, 6%) over two synthesis steps. ^{1}H NMR (MeOH-d_4): 7.79 (m, 3H), 7.34 (m, 3H), 6.37 (dd, J = 6.5, 8.3, 1H), 4.59 (m, 1H), 3.97 (m, 1H), 3.87 (dd, J = 3.5, 11.9, 1H), 3.82 (dd, J = 4.4, 11.9, 1H), 2.99 (ddd, J = 7.0, 8.3, 13.5, 1H), 2.16 (ddd, J = 2.9, 6.5, 13.5, 1H). ^{13}C NMR (MeOH-d_4): 156.89, 131.55, 131.22, 130.79, 130.39, 128.65, 128.03, 125.37, 125.04,

107.36, 106.03, 88.34, 84.31, 72.72, 63.53, 37.74. ESI-MS: M+Na^+ calc'd 323.1002, found 323.0992.

1'-β-[1-naphtho[2,3-*d*]imidazol-2(3*H*)-one)]-5'-O-(4,4'-dimethoxytrityl)-2'-deoxy-D-ribofuranose (10). Exbenzi nucleoside **5** (182 mg, 0.607 mmol) and Li_2CO_3 (215 mg, 2.91 mmol) were co-evaporated out of dichloromethane and stored overnight under vacuum. The mixture was then suspended in THF (16 mL) and diisopropylethlyamine (0.32 mL, 1.8 mmol); the nucleoside dissolved but the Li_2CO_3 remained solid (heating briefly to 50 °C did not appear to aid dissolution, as suggested by the reported procedure).(Hansen et al., 2011) DMT-BF_4 (435 mg, 1.11 mmol) was added to the stirring suspension in small portions over 6 h. At 7 h, the reaction was poured into DCM (40 mL) and washed with 50 mL each of saturated $NaHCO_3$ solution, H_2O, and saturated aqueous NaCl solution. The organics were back-extracted with an additional 50 mL DCM, and then the organics dried over Na_2SO_4 and concentrated. The material was chromatographed with a 50-100% ethyl acetate in hexanes gradient to yield the product (78 mg, 21% yield). ^{1}H NMR (acetone-d_6): 10.00 (s, 1H), 7.77 (d, J = 8.0, 1H), 7.68 (s, 1H), 7.51 (m, 2H), 7.43 (s, 1H), 7.38 (m, 4H), 7.29 (t, J = 7.4, 1H), 7.20 (m, 5H), 6.77 (m, 4H), 6.36 (m, 1H), 4.78 (m, 1H), 4.49 (d, J = 4.5, 1H), 4.08 (m, 1H), 3.70 (s, 3H), 3.68 (s, 3H), 3.43 (m, 2H), 3.09 (m, 1H), 2.18 (ddd, J = 3.5, 6.4, 13.3, 1H). ^{13}C NMR (acetone-d_6): 159.57, 159.54, 155.00, 146.15, 136.87, 136.81, 131.08, 131.00, 130.82, 130.64, 130.48, 130.37, 129.17, 128.55, 128.33, 127.60, 127.53, 124.79, 124.38, 113.84, 106.90, 105.22, 86.90, 86.35, 86.31, 83.27, 72.22, 64.85, 55.41, 55.40, 37.41. ESI-MS: M+Na^+ calc'd 625.2309, found 625.2320.

1'-β-[1-naphtho[2,3-*d*]imidazol-2(3*H*)-one)]-3'-2-cyanoethyl-tetraisopropylphosphitidyl-5'-O-(4,4'-dimethoxytrityl)-2'-deoxy-D-ribofuranose (13). DMT-protected nucleoside **10** (78 mg, 0.129 mmol) was evaporated twice out of anhydrous DCM immediately prior to use. Into the capped, N_2-flushed flask of SM was added DCM (1.5 mL), Hunig's base (0.09 mL, 0.52 mmol), and phosphoramidite reagent **12** (35 uL, 0.15 mmol), followed by a final brief flush with N_2. The reaction was allowed to proceed for 4 h; however, after 1.5 h, no further conversion of starting material was observed by TLC. The reaction mixture was then concentrated by rotatory evaporation and purified by normal-phase chromatography using a 20-50% gradient of ethyl acetate in hexanes. In addition to the desired phosphoramidite (24.6 mg, 24% yield), bis-phosphorylated material (5.6 mg,

characterized by mass spectrometry and ^{1}H NMR) and starting material (yield not determined) were recovered. ^{1}H NMR (acetone-d_6): 7.77 (d, J = 8.1, 1H), 7.70 (d, J = 6.4, 1H), 7.53 (m, 2H), 7.40 (m, 6H), 7.24 (m, 7H), 6.78 (m, 4H), 6.35 (dd, J = 2, 7, 1H), 5.01 (m, 1H), 4.21 (m, 1H), 3.74 (m, 2H), 3.70 (m, 6H), 3.66 (m, 2H), 3.50 (dd, J = 2.7, 10.4, 1H), 3.43 (ddd, J = 2.3, 4.5, 10.4, 1H), 3.22 (m, 1H), 2.62 (m, 2H), 2.33 (m, 1H), 1.21 (m, 12H). ESI-MS: M+Na$^+$ calc'd 825.3388, found 825.3405.

1*H*-naphtho[2,3-*d*]imidazole (8). According to a previously described method,(Herbert et al., 1987; Sachs, 1909) a mixture of diaminonaphthalene (1.015 g, 6.416 mmol), formic acid (4.9 mL, 130 mmol), and ethanol (10 mL) was refluxed at 85 °C under N_2 for 4.5 h. The reaction mixture was basified to pH 8 by dropwise addition of pH 13 ammonium hydroxide solution (about 10 mL). The precipitated brown solid was filtered off and washed with diethyl ether (ether washes were concentrated and resuspended to produce another batch of gold-colored product), to yield ExBIM (786 mg, 73% yield). ^{1}H NMR (MeOH-d_4): 8.39 (s, 1H), 8.08 (bs, 2H), 7.97 (m, 2H), 7.39 (m, 2H). ^{13}C NMR (MeOH-d_4): 146.99, 132.08, 129.03, 125.03. ESI-MS: M+H$^+$ calc'd 169.0760, found 169.0760.

1'-β-[1-naphtho[2,3-*d*]imidazole]-2'-deoxy-D-ribofuranose (6). The synthesis of the ExBIM nucleoside **6** was adapted from that previously described for the preparation of the Per nucleoside.(Gong and Sturla, 2007) Compound **8** (355 mg, 2.11 mmol) and anhydrous THF (24 mL) were added to a flame-dried 50 mL flask and flushed with nitrogen for several minutes. To the mixture, NaH (60% in mineral oil, 88 mg, 4.6 mmol) was added. The flask was again flushed with N_2 for several minutes, and the fine brown suspension was allowed to stir for 0.5 h. Then, chlorosugar **9** (815 mg, 2.09 mmol) was added portionwise over 4 min to the stirring suspension. After another 3.5 h stirring, the reaction was quenched with H_2O (10 mL) and concentrated by rotatory evaporation to remove the organic solvent. The remaining solution was added to DCM (50 mL) and washed with saturated $NaHCO_3$ solution (50 mL). The aqueous layer was back-extracted with an additional 50 mL DCM, and then the pooled organics were washed with an equal volume of H_2O and saturated aqueous NaCl solution and concentrated to brown syrup.

A solution of THF (40 mL), NaH (60% in mineral oil, 2 equiv), and MeOH (5 mL) was prepared and added to the crude nucleoside mixture. After 3 min, TLC indicated that the reaction was complete. The reaction mixture was filtered to remove unreacted

nucleobase, quenched with H_2O (20 mL), concentrated to a brown oil by rotatory evaporation, and purified by normal phase chromatography using a 5-10% gradient of MeOH in DCM. Target material was collected and crystallized out of MeOH/Acetone to yield a single anomer of nucleoside (188 mg, 31% yield over two synthetic steps). ^{1}H NMR (DMSO-d_6): 8.70 (s, 1H), 8.22 (m, 2H), 8.01 (m, 2H), 7.41 (m, 2H), 6.46 (dd, 6.1, 7.6, 1H), 5.37 (d, J = 4.1 Hz, 1H), 5.00 (t, J = 5.2, 1H), 4.44 (m, 1H), 3.91 (m, 1H), 3.59 (m, 2H), 2.71 (ddd, J = 6.2, 7.6, 13.3 1H), 2.35 (ddd, J = 3.1, 5.8, 13.3, 1H). ^{13}C NMR (DMSO-d_6): 146.21, 143.93, 133.36, 129.87, 129.52, 128.06, 127.54, 124.14, 123.33, 116.15, 106.98, 87.42, 84.48, 70.47, 61.48, 39.71. ESI-MS: M+H$^+$ calc'd 285.1234, found 285.1232.

1'-β-[1-naphtho[2,3-*d*]imidazole]-5'-O-(4,4'-dimethoxytrityl)-2'-deoxy-D-ribofuranose (11). ExBIM nucleoside **6** (146 mg, 0.51 mmol), Li_2CO_3 (190 mg, 2.5 mmol), THF (17 mL), and Hunig's base (0.27 mL, 1.5 mmol) were added to a flame-dried flask. (Prolonged stirring, including at 55 °C as indicated previously,(Hansen et al., 2011) did not help the reaction components to completely dissolve.) DMT-BF_4 (252 mg, 0.61 mmol) was slowly added portion-wise to the stirring suspension over 2 h. By TLC, conversion appeared to be occurring up to 6 h after reagent addition began, so the reaction was allowed to stir overnight. At 21 h, however, no further conversion was observed. The mixture was combined with DCM (40 mL) and washed with saturated $NaHCO_3$ solution. The aqueous layer was back-extracted with DCM (50 mL) and the organic layers were pooled, washed with H_2O (100 mL) and saturated aqueous NaCl solution (100 mL), and concentrated to dryness. The residue was re-suspended in DCM and filtered. The filtrate was concentrated and purified by normal phase chromatography using a 5-10% gradient of MeOH in DCM to yield target material (67 mg, 22% yield). ^{1}H NMR (acetone-d_6): 8.48 (s, 1H), 8.23 (s, 1H), 8.16 (s, 1H), 8.01 (m, 1H), 7.78 (m, 1H), 7.43 (m, 2H), 7.37 (m, 2H), 7.29 (m, 4H), 7.20 (m, 3H), 6.73 (m, 4H), 6.55 (t, J = 6.5, 1H), 4.76 (m, 1H), 4.67 (m, 1H), 4.21 (m, 1H), 3.685 (s, 3H), 3.681 (s, 3H), 3.35 (m, 2H), 2.99 (m, 1H), 2.58 (ddd, J = 4.1, 6.0, 13.4, 1H). ^{13}C NMR (acetone-d_6): 160.46, 147.31, 147.06, 146.73, 137.67, 137.62, 135.74, 132.49, 132.12, 131.92, 131.89, 130.08, 129.99, 129.52, 128.48, 126.05, 125.28, 118.65, 114.80, 109.20, 88.16, 87.92, 87.02, 73.17, 65.89, 56.38, 41.26. ESI-MS: M+Na$^+$ calc'd 609.2360, found 609.2361.

1'-β-[1-naphtho[2,3-*d*]imidazole]-3'-2-cyanoethyl-tetraisopropylphosphitidyl-5'-O-(4,4'-dimethoxytrityl)-2'-deoxy-D-ribofuranose (14). DMT-protected nucleoside **11** (67 mg, 0.115 mmol) was evaporated twice out of anhydrous DCM immediately prior to use. Into the capped, N_2-flushed flask of **11** was added DCM (1.5 mL), Hunig's base (0.08 mL, 0.46 mmol), and phosphoramidite reagent **12** (31 uL, 0.14 mmol), followed by a final brief flush with N_2. After 3 h, the reaction mixture was concentrated by rotatory evaporation and purified by normal-phase chromatography using a 25-50% gradient of ethyl acetate in hexanes. Two separate fractions of material, presumed to be each diastereomer of desired phosphoramidite, were obtained (peak A: 31.5 mg; peak B: 35.3 mg, 73% yield total). ^{1}H NMR (acetone-d_6): 8.49 (s, 1H), 8.22 (s, 1H), 8.17 (s, 1H), 8.01 (m, 1H), 7.70 (m, 1H), 7.46 (m, 2H), 7.34 (m, 6H), 7.22 (m, 3H), 6.77 (m, 4H), 6.58 (dd, J = 6.1, 7.3, 1H), 4.95 (m, 1H), 4.35 (m, 1H), 3.78 (m, 2H), 3.70 (m, 8H), 3.47 (dd, J = 3.5, 10.4), 3.40 (dd, J = 4.5, 10.4, 1H), 3.11 (m, 1H), 2.70 (ddd, J = 3.5, 5.9, 13.5, 1H), 2.66 (overlapping ts, J = 6.0, 2H), 1.22 (overlapping ds, J = 6.9, 12H). ESI-MS: M+H$^+$ calc'd 787.3619, found 787.3635.

Oligonucleotides. The oligonucleotides containing O^6-Me-G, THF, and G were purchased from the Midland Certified Reagent Company Inc. The oligonucleotides containing O^6-Bn-G and nucleoside analogs were synthesized using 5'-*O*-dimethoxytrityl protected phosphoramidites (natural nucleotides from Glen Research, Inc, and Link Technologies) on a Mermade 4 DNA synthesizer. Oligonucleotides were purified by reversed phase HPLC (Agilent 1100) on a Luna 5µm C18 (2) 100 Å 250 mm x 4.60 mm column (Phenomenex), and were eluted with acetonitrile and 50 mM triethylammonium acetate buffer using a gradient of 5% to 16% acetonitrile over 21 min. The identity of each oligonucleotide was confirmed by ESI-MS. Concentrations of oligonucleotides solutions were determined by measuring the UV absorbance at 260 nm. The molar extinction coefficients were determined via the nearest-neighbor method using the IDT calculator at http://eu.idtdna.com/analyzer/applications/oligoanalyzer. Each ε is provided in L/(mole·cm). Values used herein were: ε(5'-TTGTCGGTATAYCGG-3', where Y = G, O^6-Me-G, and O^6-Bn-G) = 145,500 (assuming that G, O^6-Me-G, and O^6-Bn-G each had the same absorbance properties), ε(5'-CCGXTATACCGACAA-3', where X = ExBIM or Exbenzi) = 152,000 (assuming that the probes have the same absorbance properties as A), and ε(5'-TTGTCGGTATAYCGG-3') = 135,600 (where Y = THF, assuming that

THF has no absorbance at 260 nm). For the dangling-end experiments, ε(5'-CGCGCG-3') = 51,400, and ε(5'-XCGCGCG-3') = 53,520 for X = Exbenzi, 53,134 for X = ExBIM, 52,260 for X = Benzi, 53,600 for X = Per, 53,900 for X = BIM, and 53,600 for X = Peri (assuming that each ε corresponds to the sum of ε(5'-CGCGCG-3') plus the ε for each free probe nucleoside, which were measured separately).

UV Melting Experiments. The melting of DNA duplexes was observed using UV spectroscopy. For non-complementary duplexes, solutions of duplex DNA (in 0.25 M NaCl, 0.2 mM EDTA, 20 mM sodium phosphate, pH 7.0 buffer) were heated (in Teflon- stoppered 1 cm path-length quartz cuvettes) to 80 °C, then cooled to 25 °C and held at that temperature for 5 minutes to anneal the duplex; then, the heating cycle was repeated to obtain the melting curve for data analysis. Two different heating/cooling rates (0.75 °C/min and 1 °C/min) were tested; no significant differences in transition temperatures due to these different rates were observed. For each probe:target duplex, measurements of at least five different concentrations (ranging from 0.8 to 10 μM) were taken. Hystereses were observed between melting and cooling curves; only melting curves were analyzed.

For dangling-end experiments, DNA solutions (of single-strand concentrations ranging from 12 to 40μM) were prepared in deionized water, then combined with equal volumes of buffer (2 M NaCl, 0.2mM EDTA, 20 mM sodium phosphate, pH 7.0) to generate sample solutions (with duplex concentrations ranging from 3 to 10 uM). These samples were heated (in Teflon- stoppered 1 cm path-length quartz cuvettes) to 90 °C, then cooled to 20 °C and held at that temperature for 25-45 min to anneal the duplex; then, the heating cycle was repeated once more to obtain a melting curve for analysis. At least five samples per duplex (with duplex concentrations ranging from 3 to 10 uM) were analyzed.

Transition Temperature Analysis. The transition temperature (T_t) of each melting curve was determined by the Cary thermal application software (using the software's derivative method), with smoothing of both the melting curve and derivative curve by 15 data points taken at 0.5 minute time increments for the non-complementary duplexes. For purposes of calculating thermodynamic parameters by evaluating the dependence of the transition temperature on duplex concentration, the transition temperatures were assumed to be approximately equal to the duplex melting temperature.

Melting Temperature Analysis. The melting temperature (T_m) of each melting curve was found using the hyperchromicity method available in the Cary Thermal application software. Briefly, the software allows the user to select upper and linear baselines for the melting curve and subsequently graphs the fraction of annealed duplex (i.e., fraction-folded, or α) vs temperature. By definition, the T_m is determined at α = 0.5.

Calculating thermodynamic parameters by evaluating the dependence of the melting transition temperature on duplex concentration. Thermodynamic parameters were derived as previously described.(Marky and Breslauer, 1987) Briefly, plots of ln C_T

$$\frac{1}{T_m} = \frac{R}{\Delta H} \ln C_T + \frac{\Delta S - R \ln 4}{\Delta H}$$

(where C_T = the total concentration of single stranded DNA) vs $1/T_m$ (or T_t) were generated. The slope and intercept of the best-fit line through the ln C_T vs $1/T_m$ (or T_t) plot were then fit into the following equation to solve for ΔH° and ΔS:

Finally, using the Gibbs equation (ΔG = ΔH − TΔS), the value of ΔG° was determined. Errors of the slope and intercept for plots of Equation 1 were determined using the LINEST function in Microsoft Excel.

Calculating thermodynamic parameters by analyzing the shape of the melting curve. Thermodynamic parameters were derived using the hyperchromicity method available in the Cary Thermal application software. Briefly, after generating a fraction-folded curve (α vs T, see "melting temperaures" above), the user then designates the linear region of the fraction-folded curve (in this work, α = 0.4-0.6 was selected for all curves). The software then plots ln K_a vs 1/T. Finally, the user designates the linear region of this curve (in this work, the regions 1/T were selected that corresponded to the upper and lower temperatures designated in the linear regions of the fraction-folded curve), and the software calculates the thermodynamic parameters of melting. Error values reported for thermodynamic parameters obtained with this method represent the standard deviation of the mean values obtained for each run.

Statistical Analysis. The ΔG° values derived from the curve-fit method were analyzed using SPSS Statistics 17.0 software. The level of significance for each analysis was

selected to be 0.05. Data sets from each probe:target duplex passed the Shapiro-Wilk test for normality; however, the data collectively failed the Levene test for homogeneity of variances (Levene statistic = 3.354, df1 = 11, df 2 = 174, sig. = 0.000). Thus, it was not possible to use the commonly-used ANOVA method for comparing the statistical differences between data sets. Instead, the Welch test for equality of means was performed; results indicated that there was a significant difference between data sets (statistic = 65.422, df1 = 11, df2 = 57.234, sig. = 0.000). Finally, the post hoc Games-Howell test (which does not require data sets of equal size or equal variance) was performed to determine the significance of differences between data sets.

Absorbance and fluorescence spectra of nucleosides and oligonucleotides. Absorbance spectra and fluorescence intensities were recorded on a Tecan infinite M200 Pro platereader. For nucleoside analogs, serial dilutions of 10% spectral grade dimethylsulfoxide (Sigma Aldrich) in water (MilliQ filtered) were prepared. For oligonucleotides 5 µM solutions in PBS buffer were prepared. Absorbance of nucleoside analogs was measured at 250 nm with a 5 nm band width in 96-well UV-Star microplates (Greiner). For fluorescence emission spectra, nucleoside analog dilutions and oligonucleotides were excited at 250 nm (5 nm band width for excitation, 20 nm band width for emission, 25°C) in black 96-well plates (Nunc).

Determination of quantum yields of nucleoside analogs. Quantum yields were determined using the comparative method of Williams *et al.*,(Williams, 1983) in which well characterized standards of a known Φ_f are used. Standards should absorb and emit fluorescence at the same wavelength as the samples to be tested (if recorded under identical conditions). The quantum yield can be calculated with the following equation:

$$\Phi_X = \Phi_{ST}\left(\frac{\mathrm{Grad}_X}{\mathrm{Grad}_{ST}}\right)\left(\frac{\eta_X^2}{\eta_{ST}^2}\right)$$

in which $\Phi_x = \Phi_f$ of sample, Φ_{ST} = literature Φ_f value of standard, Grad_x = slope of sample integrated emission intensities vs absorbance, Grad_{ST} = slope of standard integrated emission intensities vs absorbance, η^2_X = refractive index of sample solvent, and η^2_{ST} = refractive index of standard solvent. Quantum yields of nucleoside analogs (in 10% DMSO) were determined relative to standards tryptophan (Serva Feinbiochemica) in water (pH 7,) and 2-aminopyridine (Sigma Aldrich) in 0.05 M

H_2SO_4. Tryptophan has a literature quantum yield of 0.12 with an emission maxima at 356 nm (excited at 280 nm).(Chen, 1967) For 2-aminopyridine a quantum yield of 0.60 was reported (excitation wavelength 285 nm, emission between 315 – 480 nm).(Rusakowicz, 1968)

Absorbances of nucleoside analogs and standards were measured at 250 nm and plotted vs the respective concentrations of the samples (at least 5 data points). Theoretical absorbances of sample solutions at lower concentrations (i.e., those with absorbances less than 0.1) were extrapolated from the slope of the best linear fit of the absorbance *vs* concentration curves. Extrapolated values were needed for cases in which the emission intensity of higher-concentration samples exceeded the detection limit of the spectrometer. To obtain fluorescence emission spectra, samples were excited at 250 nm. To calculate the emission intensity, the area below the curve of relative fluorescence intensity was integrated (calculated using Microsoft Excel). Because the minimum emission wavelength of the platereader was set to 280 nm, the emission curves of nucleoside analogs BIM and Benzi were cut off at the lower wavelength. Therefore the integrals of fluorescence intensity for BIM and Benzi were calculated differently: the right half of the emission peak was integrated and multiplied by two. Integrated fluorescence intensities were then plotted against calculted absorbance values (at least 5 data points) and the slope of the corresponding linear trendlines were used to calculate the quantum yields with the equation above. The quantum yield of nucleoside analogs was calculated twice, using the experimentally determined slopes of each standard (tryptophan and 2-aminopyridine). Finally, the average of the two quantum yield values from both standards was used as the final value for each nucleoside analog.

Bleasdale, C., S.B. Ellwood, and B.T. Golding. 1990. Perkin communications. 4,4'-Dimethoxytrityl and 4-monomethoxytrityl tetrafluoroborate: convenient reagents for the protection of primary alcohols including sugars. J. Chem. Soc. Perk. T. 2. 0:803-805.

Brotschi, C., A. Häberli, and C.J. Leumann. 2001. A Stable DNA Duplex Containing a Non-Hydrogen-Bonding and Non-Shape-Complementary Base Couple: Interstrand Stacking as the Stability Determining Factor. Angew. Chem. Int. Ed. 40:3012-3014.

Chen, R.F. 1967. Fluorescence Quantum Yields of Tryptophan and Tyrosine. Anal Lett. 1:35-42.

de Groot, A.J.L., J.G. Jansen, C.F.M. van Valkenburg, and A.A. van Zeeland. 1994. Molecular dosimetry of 7-alkyl- and O6-alkylguanine in DNA by electrochemical detection. Mutat. Res. 307:61-66.

Dennehy, M.K., and R.N. Loeppky. 2005. Mass Spectrometric Methodology for the Determination of Glyoxaldeoxyguanosine and O6-Hydroxyethyldeoxyguanosine DNA Adducts Produced by Nitrosamine Bident Carcinogens. Chem. Res. Toxicol. 18:556-565.

Gahlon, H.L., W.B. Schweizer, and S.J. Sturla. 2013. Tolerance of Base Pair Size and Shape in Postlesion DNA Synthesis. J. Am. Chem. Soc. 135:6384-6387.

Gahlon, H.L., and S.J. Sturla. 2013a. Chem. Eur. J.

Gahlon, H.L., and S.J. Sturla. 2013b. Hydrogen Bonding or Stacking Interactions in Differentiating Duplex Stability in Oligonucleotides Containing Synthetic Nucleoside Probes for Alkylated DNA. Chem. Eur. J. 19:11062-11067.

Gao, J., H. Liu, and E.T. Kool. 2004. Expanded-Size Bases in Naturally Sized DNA: Evaluation of Steric Effects in Watson-Crick Pairing. J. Am. Chem. Soc. . 126:11826-11831.

Georgiadis, P., S. Kaila, P. Makedonopoulou, E. Fthenou, L. Chatzi, V. Pletsa, and S.A. Kyrtopoulos. 2011. Development and Validation of a New, Sensitive Immunochemical Assay for O6-Methylguanine in DNA and Its Application in a Population Study. Cancer Epidem. Biomar. 20:82-90.

Gillet, L.C.J., and O.D. Schaerer. 2002. Preparation of C8-Amine and Acetylamine Adducts of 2'-Deoxyguanosine Suitably Protected for DNA Synthesis. Org. Lett. 4:4205-4208.

Gong, J., and S.J. Sturla. 2007. A Synthetic Nucleoside Probe that Discerns a DNA Adduct from Unmodified DNA. J. Am. Chem. Soc. 129:4882-4883.

Greco, N.J., R.W. Sinkeldam, and Y. Tor. 2009. An Emissive C Analog Distinguishes between G, 8-oxoG, and T. Organic Letters. 11:1115-1118.

Greco, N.J., and Y. Tor. 2005. Simple fluorescent pyrimidine analogues detect the presence of DNA abasic sites. J. Am. Chem. Soc. 127:10784-10785.

Gresham, D. 2011. DNA Microarray-Based Mutation Discovery and Genotyping. In Methods in Molecular Biology (Molecular Methods for Evolutionary Genetics). Vol. 772. V. Orgogozo and M.V. Rockman, editors. Springer New York, NY, United States. 179-191.

Guckian, K.M., J.C. Morales, and E.T. Kool. 1998. Structure and base pairing properties of a replicable nonpolar isostere for deoxyadenosine. J. Org. Chem. 63:9652-9656.

Guckian, K.M., B.A. Schweitzer, R.X.F. Ren, C.J. Sheils, P.L. Paris, D.C. Tahmassebi, and E.T. Kool. 1996. Experimental Measurement of Aromatic Stacking Affinities in the Context of Duplex DNA. J. Am. Chem. Soc. 118:8182-8183.

Guckian, K.M., B.A. Schweitzer, R.X.F. Ren, C.J. Sheils, D.C. Tahmassebi, and E.T. Kool. 2000. Factors Contributing to Aromatic Stacking in Water: Evaluation in the Context of DNA. J. Am. Chem. Soc. 122:2213-2222.

Hansen, A.S., A. Thalhammer, A.H. El-Sagheer, T. Brown, and C.J. Schofield. 2011. Improved synthesis of 5-hydroxymethyl-2′-deoxycytidine phosphoramidite using a 2′-deoxyuridine to 2′-deoxycytidine conversion without temporary protecting groups. Bioorg. Med.Chem. Lett. 21:1181-1184.

Herbert, J.M., P.D. Woodgate, and W.A. Denny. 1987. Potential antitumor agents. 53. Synthesis, DNA binding properties, and biological activity of perimidines designed as minimal DNA-intercalating agents. J. Med. Chem. 30:2081-2086.

Huh, N.-h., M.S. Satoh, J. Shiga, M.F. Rajewsky, and T. Kuroki. 1989. Immunoanalytical Detection of O4-Ethylthymine in Liver DNA of Individuals with or without Malignant Tumors. Cancer Res. 49:93-97.

Isaksson, J., and J. Chattopadhyaya. 2005. A Uniform Mechanism Correlating Dangling-End Stabilization and Stacking Geometry†. Biochemistry. 44:5390-5401.

Kang, H.-i., C. Konishi, G. Eberle, M.F. Rajewsky, T. Kuroki, and N.-h. Huh. 1992. Highly Sensitive, Specific Detection of O6-Methylguanine, O4-Methylthymine, and O4-Ethylthymine by the Combination of High-Performance Liquid Chromatography Prefractionation, 32P Postlabeling, and Immunoprecipitation. Cancer Res. 52:5307-5312.

Kidwai, M., S. Saxena, and R. Mohan. 2005. A New Method for the Synthesis of Heterocycles from o-Phenylenediamine. J. Korean Chem. Soc. 49:288-291.

Kowal, E.A., R.R. Lad, P.S. Pallan, E. Dhummakupt, Z. Wawrzak, M. Egli, S.J. Sturla, and M.P. Stone. 2013. Recognition of O6-benzyl-2′-deoxyguanosine by a perimidinone-derived synthetic nucleoside: a DNA interstrand stacking interaction. Nucl. Acids Res.

Lai, J.S., and E.T. Kool. 2004. Selective Pairing of Polyfluorinated DNA Bases. J. Am. Chem. Soc. 126:3040-3041.

Lakshman, M.K., and B. Zajc. 1996. A Rapid, High-Yield Method for 5′-Hydroxyl Protection in Very Reactive and Amino Group Modified Nucleosides Using Dimethoxytrityl Tetrafluoroborate. Nucleos. Nucleot. 15:1029-1039.

Lazar, Z., B. Benali, K. Elblidi, M. Zenkouar, B. Lakhrissr, M. Massoui, B. Kabouchi, and C. Cazeau-Dubroca. 2003. Photophysical study of benzimidazolone and its derivative molecules in solution. J Mol Liq. 106:89-95.

Lee, A.H.F., and E.T. Kool. 2005. Novel Benzopyrimidines as Widened Analogues of DNA Bases. J. Org. Chem. 70:132-140.

Lee, H., E. Luna, M. Hinz, J.J. Stezowski, A.S. Kiselyo, and R.G. Harvey. 1995. Synthesis of Oligonucleotide Adducts of the Bay Region Diol Epoxide Metabolites of Carcinogenic Polycyclic Aromatic Hydrocarbons. J. Org. Chem. 60:5604-5613.

Lindahl, T. 1993. Instability and decay of the primary structure of DNA. Nature. 362:709-715.

Liu, H., J. Gao, and E.T. Kool. 2005. Size-Expanded Analogues of dG and dC: Synthesis and Pairing Properties in DNA. J. Org. Chem. 70:639-647.

Lu, H., K. He, and E.T. Kool. 2004. yDNA: A New Geometry for Size-Expanded Base Pairs Angew. Chem. Int. Ed. 43:5834 –5836.

Margison, G.P., M.F. Santibáñez Koref, and A.C. Povey. 2002. Mechanisms of carcinogenicity/chemotherapy by O6-methylguanine. Mutagenesis. 17:483-487.

Marky, L.A., and K.J. Breslauer. 1987. Calculating thermodynamic data for transitions of any molecularity from equilibrium melting curves. Biopolymers. 26:1601-1620.

McCullough, A.K., M.L. Dodson, O.D. Schärer, and R.S. Lloyd. 1997. The role of base-flipping in damage recognition and catalysis by T4 endonuclease V. J. Biol. Chem. 272:27210-27217.

Morales-Rojas, H., and E.T. Kool. 2002. A Porphyrin C-Nucleoside Incorporated into DNA. Organic Letters. 4:4377-4380.

Mounetou, E., E. Debiton, C. Buchdahl, D. Gardette, J.-C. Gramain, J.-C. Maurizis, A. Veyre, and J.-C. Madelmont. 1997. O6-(Alkyl/aralkyl)guanosine and 2‘-

Deoxyguanosine Derivatives: Synthesis and Ability To Enhance Chloroethylnitrosourea Antitumor Action. J. Med. Chem. 40:2902-2909.

Nakano, S.-i., M. Fujii, and N. Sugimoto. 2011. Use of Nucleic Acid Analogs for the Study of Nucleic Acid Interactions. Journal of Nucleic Acids. 2011.

Nasr, T., Z. Li, O. Nakagawa, Y. Taniguchi, S. Ono, and S. Sasaki. 2009. Selective fluorescence quenching of the 8-oxoG-clamp by 8-oxodeoxyguanosine in ODN. Bioorganic & Medicinal Chemistry Letters. 19:727-730.

Nazar, R.N., and J. Robb. 2012. DNA Chip Analysis in Genome Discovery. In Molecular Analysis and Genome Discovery, Second Edition. R. Raphley and S. Harbron, editors. John Wiley & Sons, Ltd.

Ogawa, A.K., Y. Wu, D.L. McMinn, J. Liu, P.G. Schultz, and F.E. Romesberg. 2000. Efforts toward the Expansion of the Genetic Alphabet: Information Storage and Replication with Unnatural Hydrophobic Base Pairs. J. Am. Chem. Soc. 122:3274-3287.

Onizuka, K., T. Nishioka, Z. Li, D. Jitsuzaki, Y. Taniguchi, and S. Sasaki. 2012. An efficient and simple method for site-selective modification of O6-methyl-2'-deoxyguanosine in DNA. Chem. Comm. 48:3969-3971.

Pegg, A.E., M.E. Dolan, R.C. Moschel, E.C. Waldo, and M. Kivie. 1995. Structure, function, and inhibition of O6-alkylguanine-DNA alkyltransferase. In Progress in Nucleic Acid Research and Molecular Biology. Vol. Volume 51. Academic Press. 167-223.

Rachofsky, E.L., E. Seibert, J.T. Stivers, R. Osman, and J.B.A. Ross. 2001. Conformation and Dynamics of Abasic Sites in DNA Investigated by Time-Resolved Fluorescence of 2-Aminopurine†. Biochemistry. 40:957-967.

Reh, B.D., D.G. DeBord, M.A. Butler, T.M. Reid, C. Mueller, and J.M. Fajen. 2000. O6-methylguanine DNA adducts associated with occupational nitrosamine exposure. Carcinogenesis. 21:29-33.

Roday, S., M.B. Sturm, D.M. Blakaj, and V.L. Schramm. 2008. Detection of an abasic site in RNA with stem-loop DNA beacons: Application to an activity assay for Ricin Toxin A-Chain. J. Biochem. Bioph. Meth. 70:945-953.

Rosemeyer, H., and F. Seela. 2002. Modified purine nucleosides as dangling ends of DNA duplexes: the effect of the nucleobase polarizability on stacking interactions. J. Chem. Soc., Perkin Trans. 2:746–750.

Rusakowicz, R.T., A. C. 1968. 2-Aminopyridine as a standard for low-wavelength spectrofluorimetry. J Phys Chem. 72:2680-2681.

Sachs, F. 1909. Ueber Ringschlüsse in Peristellung der Naphtalinreihe. Liebigs Ann.Chem. 365:53-134.

Sealfon, S.C., and T.T. Chu. 2011. RNA and DNA Microarrays. In Biological Microarrays: Methods and Protocols. Vol. 671. A.K.e. al., editor. Springer. 3-34.

Shipova, E., and K.S. Gates. 2005. A fluorimetric assay for the spontaneous release of an N7-alkylguanine residue from duplex DNA. Bioorg. Med. Chem. Lett. 15:2111-2113.

Sinkeldam, R.W., N.J. Greco, and Y. Tor. 2010. Fluorescent analogs of biomolecular building blocks: design, properties, and applications. Chemical reviews. 110:2579-2619.

Stivers, J.T. 1998. 2-Aminopurine fluorescence studies of base stacking interactions at abasic sites in DNA: metal-ion and base sequence effects. Nuc. Acids. Res. 26:3837-3844.

Wang, D.G., J.-B. Fan, C.-J. Siao, A. Berno, P. Young, R. Sapolsky, G. Ghandour, N. Perkins, E. Winchester, J. Spencer, L. Kruglyak, L. Stein, L. Hsie, T. Topaloglou, E. Hubbell, E. Robinson, M. Mittmann, M.S. Morris, N. Shen, D. Kilburn, J. Rioux, C. Nusbaum, S. Rozen, T.J. Hudson, R. Lipshutz, M. Chee, and E.S. Lander. 1998. Large-Scale Identification, Mapping, and Genotyping of Single-Nucleotide Polymorphisms in the Human Genome. Science. 280:1077-1082.

Wang, L., and P.C.H. Li. 2011. Microfluidic DNA microarray analysis: A review. Analytica Chimica Acta. 687:12-27.

Wilhelmsson, L.M. 2010. Fluorescent nucleic acid base analogues. Quarterly Reviews of Biophysics. 43:159-183.

Williams, A.T.R.W., S. A.; Miller, J. N. 1983. Relative fluorescence quantum yields using a computer-controlled luminescence spectrometer. The Analyst:1067-1071.

Wu, Y., A.K. Ogawa, M. Berger, D.L. McMinn, P.G. Schultz, and F.E. Romesberg. 2000. Efforts toward Expansion of the Genetic Alphabet: Optimization of Interbase Hydrophobic Interactions. J. Am. Chem. Soc. 122:7621-7632.

Wyatt, M.D., and D.L. Pittman. 2006. Methylating agents and DNA repair responses: methylated bases and sources of strand breaks. Chem. Res. Toxicol. 19:1580-1594.

Yang, Y., D. Nikolic, S.M. Swanson, and R.B. van Breemen. 2002. Quantitative Determination of N7-Methyldeoxyguanosine and O6-Methyldeoxyguanosine in DNA by LC–UV–MS–MS. Anal. Chem. 74:5376-5382.

Example 2

Assay principle. The nanoparticle-based detection system discussed herein involves two different oligonucleotide-modified AuNP probes that align in a tail-to-tail fashion onto a complementary target oligonucleotide (Fig. 5b). Two sets of AuNPs (d=20 nm) were functionalized with 5'-thiol-modified (probe 1, Table 5) or 3'-thiol-modified (probe 2, Table 5) oligonucleotides, respectively. Probe 1 was a 16-mer consisting of an $(A)_{10}$ spacer and a 6-mer recognition sequence. Probe 2 was a 17-mer consisting of an $(A)_{10}$ spacer and a 7-mer recognition sequence and the first base at the 5'-end was ExBIM. The 13-base oligonucleotide target strand was designed to have its 5'-end complementary to the 3'-end of probe 1, and its 3'-end complementary to the 5'-end of probe 2. The target could cross-link the two distinct sets of AuNPs through hybridization, forming an aggregate network of AuNPs. Dispersed functionalized 20-nm AuNPs have an intense red color due to the localized surface plasmon resonance (SPR) and exhibit a characteristic SPR band at 530 nm (Fig. 6). The close proximity of the cross-linked AuNPs caused coupling of their individual localized plasmon fields, leading to a shift in their absorbance to a longer wavelength, and the color of the solution changed from red to purple. Therefore, upon addition of target the 530-nm SPR peak decreased while the absorbance in the 700-nm region increased (Fig. 6). The absorbance ratio at 700 nm vs. 530 nm was used for characterizing the aggregation state.

Table 5. Oligonucleotide sequences used in this study

The underlined bases denote the recognition sequences, P = ExBIM, X = O^6-meG

Name	Sequence
Probe 1	5 '- HS - $(A)_{10}$ CCTACG - 3'
Probe 2	5' - PCACCAG $(A)_{10}$ - SH - 3'
Probe 3	5' - CCTACGPCACCAG - 3'
O^6-meG target	5' - CTGGTGXCGTAGG - 3'
G target	5' - CTGGTGGCGTAGG - 3'
Irrelevant target	5' - CCCATCCACCCAC - 3'

Specificity studies. The specificity of the AuNP probes was assessed by using as target synthetic oligonucleotides that were designed to represent a mutational hotspot codon in exon 2 of the K-ras oncogene. The *RAS* gene family is among the most studied and best characterized of the known cancer-related genes. The *RAS* oncogene is well established to influence cell growth and regulation; its protein product affects cell proliferation, apoptosis, migration, fate specification, and differentiation. There are three known human isoforms: *NRAS*, *HRAS*, and *KRAS*. Of the three human ras isoforms, *KRAS* is the most frequently altered gene, with mutations occurring in 17%–25% of all cancers. In particular, approximately 30%–40% of colon cancers harbor a *KRAS* mutation. *KRAS* mutations in colon cancers have been associated with poorer survival and increased tumor aggressiveness. Additionally, *KRAS* mutations in colorectal cancer lead to resistance to select treatment strategies. KRAS mutations in exon 2 (codons 12 and 13), and to a lesser extent in exon 3 (codon 61), are associated with colorectal cancer outcome. Nearly 97% of all KRAS mutations are considered an early event in the adenoma-carcinoma sequence and are localized to codons 12 or 13, with a large majority located in codon 12[28]. Mutations in each of the three codons compromise the ability of GTPase-activating proteins to inactivate hydrolysis of Ras-bound GTP to GDP[29]. Other mutations are uncommon as they result in lower constitutive Ras signaling than mutations in codons 12, 13 and 61, and so are selected against in carcinogenesis[30].

Specifically, the target oligonucleotides (13-mers) were designed so that the middle base would correspond to the K-ras codon 13 mutational hotspot (Table 5). The target

oligomers varied in the identity of the base placed opposite ExBIM. This position was at the centre of the target sequence to achieve highest discrimination between the adduct and the natural base, as it was shown by previous studies concerning mismatch discrimination[45-47]. Thus we tested as targets: 1) an oligonucleotide containing the alkylated base O^6-meG and 2) an oligonucleotide containing the natural base G. Additionally, we synthesized a non-complementary 13-mer sequence (Table 1, irrelevant target) as a negative control.

To evaluate the stability of the aggregates formed in the presence of different target oligonucleotides we compared the melting temperatures (T_m) of AuNP probes containing ExBIM paired opposite O^6-meG or control sequences. This melting analysis was performed by monitoring the absorbance of the solution with the re-suspended aggregates at 530 nm as a function of temperature and measured the transition from the aggregate to the dispersed state of the AuNP probes. This transition reflects the hybridization state of the 3-component system comprised of the target oligonucleotide and the tails of the NP-bound DNA sequences.

Thus, the T_m of the aggregates formed from the AuNP probes and 20 nM (Fig. 7a) of the O^6-meG-containing target was 32.7 °C. For the same AuNP probe and target concentration, the T_m values for aggregates formed from the G- containing target was 29.4 °C. Therefore the difference in the melting temperatures (ΔT_m) between the aggregates formed from the O^6-meG and G containing targets was 3.3 °C.

Dissociation curves were also obtained for DNA duplexes formed from the different targets and the conventional oligonucleotide Probe 3 whose sequence combines the recognition sequences of Probes 1 and 2. Higher concentrations of oligomers (2.2 μM in each oligonucleotide) were used in order to obtain a measurable signal at 260 nm; the experiment could not be performed at concentrations comparable to those used for the aforementioned nanoparticle probe studies since the conventional oligonucleotides do not exhibit measurable absorbance changes upon hybridization in this concentration range. Broad melting curves were observed in all these cases, with T_m values of 54.0 and 51.7 °C when ExBIM was placed opposite O^6-meG and G, respectively.

Specificity studies in mixtures of targets. To address the specificity of this system regarding whether DNA adducts could be detected as a minority component in a mixture of oligonucleotides, we performed a competition experiment to assess the

ability of the O^6-meG-containing target to increase the thermal stability of the aggregates in the presence of other targets that can also induce aggregation (Table 5). In particular, three solutions of aggregates were tested. Each contained the two AuNP probes (1 nM each) and 2 pmol of each of the G and irrelevant target (20 nM each, final concentration). To one of the solutions, 2 pmol of the O^6-meG- containing target was added (20 nM final concentration), and to another one 2 pmol of the G containing target (40 nM final concentration). Therefore the total target concentration for both solutions was the same (60 nM). The third solution, where no extra target was added, served as a control. Furthermore, a mixture of the two AuNP probes where no target was added served as a negative control for aggregation. Upon aggregation, the solutions were heated for 5 min at different temperatures (25-41 °C). The absorbance ratio (A_{700}/A_{530}), reflecting aggregation state, decreased at higher temperatures, indicating dispersion of the aggregates. However the rate of dispersion for O^6-meG- was slower than for G-supplemented solutions (Fig. 7A). In order to assess in this mixture the discrimination efficiency of ExBIM between O^6-meG and G we determined the difference in absorbance ratios $\Delta(A_{700}/A_{530})$, between the O^6-meG- and G-supplemented solutions as a function of temperature (Fig. 3B). The $\Delta(A_{700}/A_{530})$ ranged between 0.05 and 0.44. The maximum discrimination ($\Delta(A_{700}/A_{527}) = 0.44$) was observed at 27 °C. This experiment demonstrates that the proposed nanoprobes can discriminate alkylated targets in a mixture with unmodified sequences that are the same but contain a G.

Characterization of sensitivity. In order to assess the sensitivity of this ratiometric detection assay, solutions of aggregates were formed by mixing the two AuNP probes (1 nM each) with a mixture of the G and irrelevant target (20 nM each, final concentration). The nanoprobe-target mixtures were then further supplemented with O^6-meG/G target solutions , in which the relative concentration of O^6-meG ranged from 0 to 25 %. Upon aggregation, the absorbance ratio (A_{700}/A_{530}) was determined. Under these conditions, A_{700}/A_{530} values decreased linearly ($R^2 = 0.990$) as the relative concentration of O^6-meG decreased from 25% to 0%, indicating a corresponding decrease in aggregate stability (Fig.8A). Additionally, the detection limit for this assay was 96 fmol of the O^6-meG-containing target (0.96 nM) in the presence of 4 pmol of the G target (40 nM), which corresponds to a relative O^6-meG-containing target concentration of 2.4 % (Fig. 8A).

Furthermore, when the presence of the irrelevant target is taken into account, the detection limit for this assay was 96 fmol of the O^6-meG target (0.96 nM) in the presence of 6 pmol of total DNA targets (60 nM), which corresponds to a relative O^6-meG-containing target concentration of 1.6 %.(Fig. 8B)

References

1 Liao, Q. & Vouros, P. in *Advances in Chromatography, Vol 49* Vol. 49 *Advances in Chromatography* (eds E. Grushka & N. Grinberg) 195-256 (Crc Press-Taylor & Francis Group, 2011).

2 Rundle, A. Carcinogen-DNA adducts as a biomarker for cancer risk. *Mutat. Res.-Fundam. Mol. Mech. Mutagen.* **600**, 23-36, doi:10.1016/j.mrfmmm.2006.05.031 (2006).

3 Hemminki, K., Koskinen, M., Rajaniemi, H. & Zhao, C. Y. DNA adducts, mutations, and cancer 2000. *Regul. Toxicol. Pharmacol.* **32**, 264-275, doi:10.1006/rtph.2000.1431 (2000).

4 Klaene, J. J., Sharma, V. K., Glick, J. & Vouros, P. The analysis of DNA adducts: The transition from (32)P-postlabeling to mass spectrometry. *Cancer Lett*, doi:10.1016/j.canlet.2012.08.007 (2012).

5 Garner, R. C. The role of DNA adducts in chemical carcinogenesis. *Mutat. Res.-Fundam. Mol. Mech. Mutagen.* **402**, 67-75 (1998).

6 Otteneder, M. & Lutz, W. K. Correlation of DNA adduct levels with tumor incidence: carcinogenic potency of DNA adducts. *Mutation Research/Fundamental and Molecular Mechanisms of Mutagenesis* **424**, 237-247, doi:http://dx.doi.org/10.1016/S0027-5107(99)00022-6 (1999).

7 Wild, C. P. Environmental exposure measurement in cancer epidemiology. *Mutagenesis* **24**, 117-125, doi:10.1093/mutage/gen061 (2009).

8 Delaney, J. C. & Essigmann, J. M. Context-dependent mutagenesis by DNA lesions. *Chem. Biol.* **6**, 743-753, doi:10.1016/s1074-5521(00)80021-6 (1999).

9 Denissenko, M. F., Pao, A., Tang, M. S. & Pfeifer, G. P. Preferential formation of benzo a pyrene adducts at lung cancer mutational hotspots in P53. *Science* **274**, 430-432, doi:10.1126/science.274.5286.430 (1996).

10 Delaney, J. C. & Essigmann, J. M. Effect of sequence context on O-6-methylguanine repair and replication in vivo. *Biochemistry* **40**, 14968-14975, doi:10.1021/bi015578f (2001).

11 Koivisto, P. & Peltonen, K. Analytical methods in DNA and protein adduct analysis. *Analytical and Bioanalytical Chemistry* **398**, 2563-2572, doi:10.1007/s00216-010-4217-3 (2010).

12 Kyrtopoulos, S. A., Ampatzi, P., Davaris, P., Haritopoulos, N. & Golematis, B. Studies in gastric carcinogenesis. IV. O6-Methylguanine and its repair in normal and atrophic biopsy specimens of human gastric mucosa. Correlation of O6-alkylguanine-DNA alkyltransferase activities in gastric mucosa and circulating lymphocytes. *Carcinogenesis* **11**, 431-436, doi:10.1093/carcin/11.3.431 (1990).

13 Badawi, A. F. *et al.* Promutagenic methylation damage in bladder DNA from patients with bladder cancer associated with schistosomiasis and from normal individuals. *Carcinogenesis* **13**, 877-881, doi:10.1093/carcin/13.5.877 (1992).

14 Kang, H.-i., Konishi, C., Kuroki, T. & Huh, N.-h. Detection of O6-methylguanine, O4-methylthymine and O4-ethylthymine in human liver and peripheral blood leukocyte DNA. *Carcinogenesis* **16**, 1277-1280, doi:10.1093/carcin/16.6.1277 (1995).

15 Szyfter, K. *et al.* Tobacco smoke-associated N7-alkylguanine in DNA of larynx tissue and leucocytes. *Carcinogenesis* **17**, 501-506, doi:10.1093/carcin/17.3.501 (1996).

16 Mustonen, R., Schoket, B. & Hemminki, K. Smoking-related DNA adducts: 32P-postlabeling analysis of 7-methylguanine in human bronchial and lymphocyte DNA. *Carcinogenesis* **14**, 151-154, doi:10.1093/carcin/14.1.151 (1993).

17 Rossi, S. C., Conrad, M., Voigt, J. M. & Topal, M. D. Excision repair of O6-methylguanine synthesized at the rat H-ras N-methyl-N-nitrosourea activation site and introduced into Escherichia coli. *Carcinogenesis* **10**, 373-377, doi:10.1093/carcin/10.2.373 (1989).

18 Pletsa, V., Troungos, C., Souliotis, V. L. & Kyrtopoulos, S. A. Comparative study of mutagenesis by O6-methylguanine in the human Ha-ras oncogene in E.coli and in vitro. *Nucleic Acids Research* **22**, 3846-3853, doi:10.1093/nar/22.19.3846 (1994).

19 Tan, H.-B., Swann, P. F. & Chance, E. M. Kinetic Analysis of the Coding Properties of O6-Methylguanine in DNA: The Crucial Role of the Conformation of the Phosphodiester Bond. *Biochemistry* **33**, 5335-5346, doi:10.1021/bi00183a042 (1994).

20 Mirsalis, J. C., Monforte, J. A. & Winegar, R. A. Transgenic Animal Models for Measuring MutationsIn Vivo. *Critical Reviews in Toxicology* **24**, 255-280, doi:doi:10.3109/10408449409021608 (1994).

21 Swenberg, J. A., Bedell, M. A., Billings, K. C., Umbenhauer, D. R. & Pegg, A. E. Cell-specific differences in O6-alkylguanine DNA repair activity during continuous exposure to carcinogen. *Proceedings of the National Academy of Sciences* **79**, 5499-5502 (1982).

22 Povey, A. C. *et al.* DNA Alkylation and Repair in the Large Bowel: Animal and Human Studies. *The Journal of Nutrition* **132**, 3518S-3521S (2002).

23 Wolf, P., Hu, Y. C., Doffek, K., Sidransky, D. & Ahrendt, S. A. O6-Methylguanine-DNA Methyltransferase Promoter Hypermethylation Shifts the p53 Mutational Spectrum in Non-Small Cell Lung Cancer. *Cancer Research* **61**, 8113-8117 (2001).

24 Wu, J.-Y. *et al.* Association of O6-Methylguanine-DNA Methyltransferase (MGMT) Promoter Methylation with p53 Mutation Occurrence in Non-Small Cell Lung Cancer with Different Histology, Gender, and Smoking Status. *Ann Surg Oncol* **15**, 3272-3277, doi:10.1245/s10434-008-0078-9 (2008).

25 Pegg, A. E. Mammalian O6-Alkylguanine-DNA Alkyltransferase: Regulation and Importance in Response to Alkylating Carcinogenic and Therapeutic Agents. *Cancer Research* **50**, 6119-6129 (1990).

26 Kyrtopoulos, S. A. DNA adducts in humans after exposure to methylating agents. *Mutation Research/Fundamental and Molecular Mechanisms of Mutagenesis* **405**, 135-143, doi:http://dx.doi.org/10.1016/S0027-5107(98)00130-4 (1998).

27 Mirvish, S. S. Role of N-nitroso compounds (NOC) and N-nitrosation in etiology of gastric, esophageal, nasopharyngeal and bladder cancer and contribution to cancer of known exposures to NOC. *Cancer Letters* **93**, 17-48, doi:http://dx.doi.org/10.1016/0304-3835(95)03786-V (1995).

28 Andreyev, H. J. N., Norman, A. R., Clarke, P. A., Cunningham, D. & Oates, J. R. Kirsten ras Mutations in Patients With Colorectal Cancer: the Multicenter "RASCAL" Study. *Journal of the National Cancer Institute* **90**, 675-684, doi:10.1093/jnci/90.9.675 (1998).

29 Downward, J. Targeting RAS signalling pathways in cancer therapy. *Nat Rev Cancer* **3**, 11-22 (2003).

30 Wolpin, B. M. & Mayer, R. J. Systemic Treatment of Colorectal Cancer. *Gastroenterology* **134**, 1296-1310.e1291, doi:http://dx.doi.org/10.1053/j.gastro.2008.02.098 (2008).

31 Foiles, P. G., Miglietta, L. M., Akerkar, S. A., Everson, R. B. & Hecht, S. S. Detection of O6-Methyldeoxyguanosine in Human Placental DNA. *Cancer Research* **48**, 4184-4188 (1988).

32 Haque, K., Cooper, D. P., van Delft, J. H. M., Lee, S. M. & Povey, A. C. Accurate and Sensitive Quantitation of N7-Methyldeoxyguanosine-3'-monophosphate by 32P-Postlabeling and Storage-Phosphor Imaging. *Chemical Research in Toxicology* **10**, 660-666, doi:10.1021/tx9601723 (1997).

33 O6-Methylguanine in blood leucocyte DNA: an association with the geographic prevalence of gastric cancer and with low levels of serum pepsinogen A, a marker of severe chronic atrophic gastritis. *Carcinogenesis* **15**, 1815-1820, doi:10.1093/carcin/15.9.1815 (1994).

34 Georgiadis, P., Samoli, E., Kaila, S., Katsouyanni, K. & Kyrtopoulos, S. A. Ubiquitous Presence of O6-Methylguanine in Human Peripheral and Cord Blood DNA. *Cancer Epidemiology Biomarkers & Prevention* **9**, 299-305 (2000).

35 Georgiadis, P. *et al.* Development and Validation of a New, Sensitive Immunochemical Assay for O6-Methylguanine in DNA and Its Application in a Population Study. *Cancer Epidemiology Biomarkers & Prevention* **20**, 82-90, doi:10.1158/1055-9965.epi-10-0788 (2011).

36 Gong, J. & Sturla, S. J. A Synthetic Nucleoside Probe that Discerns a DNA Adduct from Unmodified DNA. *J. Am. Chem. Soc.* **129**, 4882-4883, doi:10.1021/ja070688g (2007).

37 Gahlon, H. L. & Sturla, S. J. Hydrogen Bonding or Stacking Interactions in Differentiating Duplex Stability in Oligonucleotides Containing Synthetic Nucleoside Probes for Alkylated DNA. *Chem. Eur. J.* **19**, 11062-11067, doi:10.1002/chem.201204593 (2013).

38 Gong, J. C. & Sturla, S. J. A synthetic nucleoside probe that discerns a DNA adduct from unmodified DNA. *Journal of the American Chemical Society* **129**, 4882-+, doi:10.1021/ja070688g (2007).

39 Baptista, P. *et al.* Gold nanoparticles for the development of clinical diagnosis methods. *Analytical and Bioanalytical Chemistry* **391**, 943-950, doi:10.1007/s00216-007-1768-z (2008).

40 Cao, X., Ye, Y. & Liu, S. Gold nanoparticle-based signal amplification for biosensing. *Analytical Biochemistry* **417**, 1-16, doi:http://dx.doi.org/10.1016/j.ab.2011.05.027 (2011).

41 Jain, P. K., Lee, K. S., El-Sayed, I. H. & El-Sayed, M. A. Calculated Absorption and Scattering Properties of Gold Nanoparticles of Different Size, Shape, and Composition: Applications in Biological Imaging and Biomedicine. *The Journal of Physical Chemistry B* **110**, 7238-7248, doi:10.1021/jp057170o (2006).

42 Khlebtsov, N. G., Trachuk, L. A. & Mel'nikov, A. G. The effect of the size, shape, and structure of metal nanoparticles on the dependence of their optical properties on the refractive index of a disperse medium. *Opt. Spectrosc.* **98**, 77-83, doi:10.1134/1.1858043 (2005).

43 Bao, Y. P. *et al.* SNP identification in unamplified human genomic DNA with gold nanoparticle probes. *Nucleic Acids Research* **33**, e15, doi:10.1093/nar/gni017 (2005).

44 Park, S.-J., Taton, T. A. & Mirkin, C. A. Array-Based Electrical Detection of DNA with Nanoparticle Probes. *Science* **295**, 1503-1506, doi:10.1126/science.1067003 (2002).

45 Huber, F., Lang, H. P., Backmann, N., Rimoldi, D. & Gerber, C. Direct detection of a BRAF mutation in total RNA from melanoma cells using cantilever arrays. *Nature Nanotechnology* **8**, 125-129, doi:10.1038/nnano.2012.263 (2013).

46 Doria, G., Baumgartner, B. G., Franco, R. & Baptista, P. V. Optimizing Au-nanoprobes for specific sequence discrimination. *Colloids and Surfaces B: Biointerfaces* **77**, 122-124, doi:http://dx.doi.org/10.1016/j.colsurfb.2010.01.007 (2010).

47 Zhang, D. Y., Chen, S. X. & Yin, P. Optimizing the specificity of nucleic acid hybridization. *Nat Chem* **4**, 208-214, doi:http://www.nature.com/nchem/journal/v4/n3/abs/nchem.1246.html#supplementary-information (2012).

Example 3 Enrichment/isolation of DNA adducts in Kras

DNA is isolated from a biological sample (e.g., stool, blood, or tissue) and is subjected to digestion with a restriction enzyme that digests the Kras gene upstream and downstream of a DNA adduct hotspot.

Digested DNA is mixed with biotinylated oligonucleotides that are designed to hybridize with the DNA fragments of the mutational hotspot. These biotinylated oligos also comprise ExBIM or Exbenzi.

Biotinylated hybrids are mixed with Streptavidin coated magnetic beads (e.g. Dynabeads® from Invitrogen).

The biotinylated hybrids are captured on the magnetic beads through biotin-streptavidin interaction.

Magnetic field is applied so that hybrids are separated from unhybridized DNA fragments.

Solution is discarded and captured targets are washed with water or appropriate buffer to remove any residual unhybridized targets.

Magnetic beads are resuspended in water or appropriate buffer. Dispersion is briefly heated (e.g. 5 min at 70 °C), so that the hybrid duplex is denatured.

Magnetic field is applied while dispersion is still heated. The biotinylated capture probes stay on the magnetic beads (the biotin-streptavidin interaction is very strong and not affected by short-term heating in aqueous solutions).

The target polynucleotide fragments are in solution and can be collected.

Claims

1. An oligonucleotide comprising at least one base-modified-nucleotide analog wherein the base-modified-nucleotide comprises the following structure:

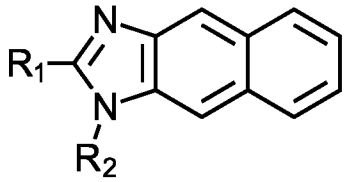

wherein R1 is selected from OH or H; and R2 is selected from a deoxyribose moiety of a polynucleotide, a ribose moiety of a polynucleotide, and a nucleic acid backbone mimic moiety.

2. The oligonucleotide of claim 1, wherein R1 is OH.

3. A base-modified-nucleoside analog having the following structure:

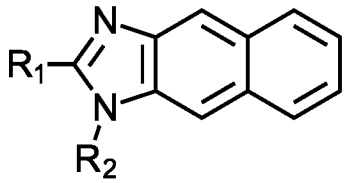

wherein R1 is OH and R2 is selected from a ribose moiety, a deoxyribose moiety, and a nucleic acid backbone mimic moiety or

R1 is H and R2 is selected from a deoxyribose moiety and a nucleic acid backbone mimic moiety.

4. The base modified nucleoside analog of claim 3 having the following structure:

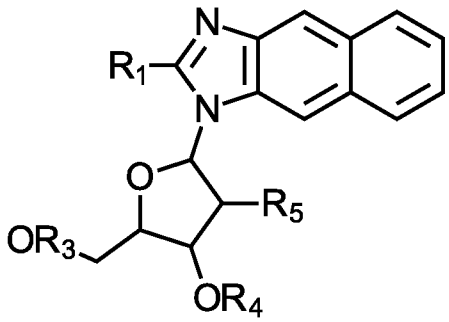

wherein R3 is selected from H, phosphorothioate monophosphate, (PO_3), $(PO_3)_2$, $(PO_3)_3$, and a protective group for a hydroxyl group for synthesis of nucleic acid, and R4 is selected from H, a protective group for a hydroxyl group for synthesis of nucleic acid, a phosphate group, a phosphate group protected with a protective group for synthesis of nucleic acid, or -P(R7)R8 [where R7 and R8 are identical or different, and each represent a hydroxyl group, a hydroxyl group protected with a protective group for synthesis of nucleic acid, a mercapto group, a mercapto group protected with a protective group for synthesis of nucleic acid, an amino group, an alkoxy group having 1 to 5 carbon atoms, an alkylthio group having 1 to 5 carbon atoms, a cyanoalkoxy group having 1 to 6 carbon atoms, or a primary or secondary amine substituted by an alkyl group having 1 to 5 carbon atoms], and
R5 is selected from H, OH, O-alkyl(Cl-C6), F, CI, NH2, CN, SH, and a 2'- 4' bridge locking the sugar in the C3 endo configuration, wherein R5 is not OH when R1 is H.

5. The base modified nucleoside analog of claim 3 or 4, where R1 is OH.

6. The use of an oligonucleotide according to any one of claims 1-2 or a base modified nucleoside analog according to any one of claims 3-5 for detecting the presence of O^6-alkyl guanine.

7. The use of an oligonucleotide according to any one of claims 1-2 for isolating a polynucleotide comprising O^6-alkyl guanine.

8. A method for detecting the presence of O^6-alkyl guanine in a target polynucleotide, said method comprising a) contacting the target polynucleotide with a first oligonucleotide according to any one of claims 1-2 that is complementary to said

polynucleotide such that said polynucleotide and said first oligonucleotide form a target duplex and b) measuring the formation of said duplex.

9. The method according to claim 8, further comprising contacting said target polynucleotide with a second oligonucleotide that is complementary to said polynucleotide such that said polynucleotide can simultaneously hybridize to both the first and second oligonucleotides forming a duplex and b) measuring the formation of said duplex.

10. The method according to claim 8, further comprising contacting said target polynucleotide with a second oligonucleotide that is complementary to said first oligonucleotide such that said second oligonucleotide competes with the target polynucleotide for binding to the first oligonucleotide.

11. The method of any one of claims 8-10, wherein the first and/or second oligonucleotide is attached to a solid substrate.

12. A method for isolating an O^6-alkyl guanine containing target polynucleotide, said method comprising a) contacting a nucleic acid containing sample with an oligonucleotide according to claim 1 or 2, wherein said oligonucleotide is complementary to said target polynucleotide such that said target polynucleotide and said oligonucleotide form a target duplex and b) isolating said target duplex.

13. The use of claims 6 or 7 and the method of any one of claims 8-12, wherein said O^6-alkyl guanine is O^6-methyl guanine.

14. A kit of parts comprising a solid substrate, preferably particles, more preferably gold nanoparticles, and an oligonucleotide according to any one of 1-2.

15. An oligonucleotide according to any one of 1-2 immobilized to a solid substrate, preferably particles, more preferably gold nanoparticles.

Figure 1

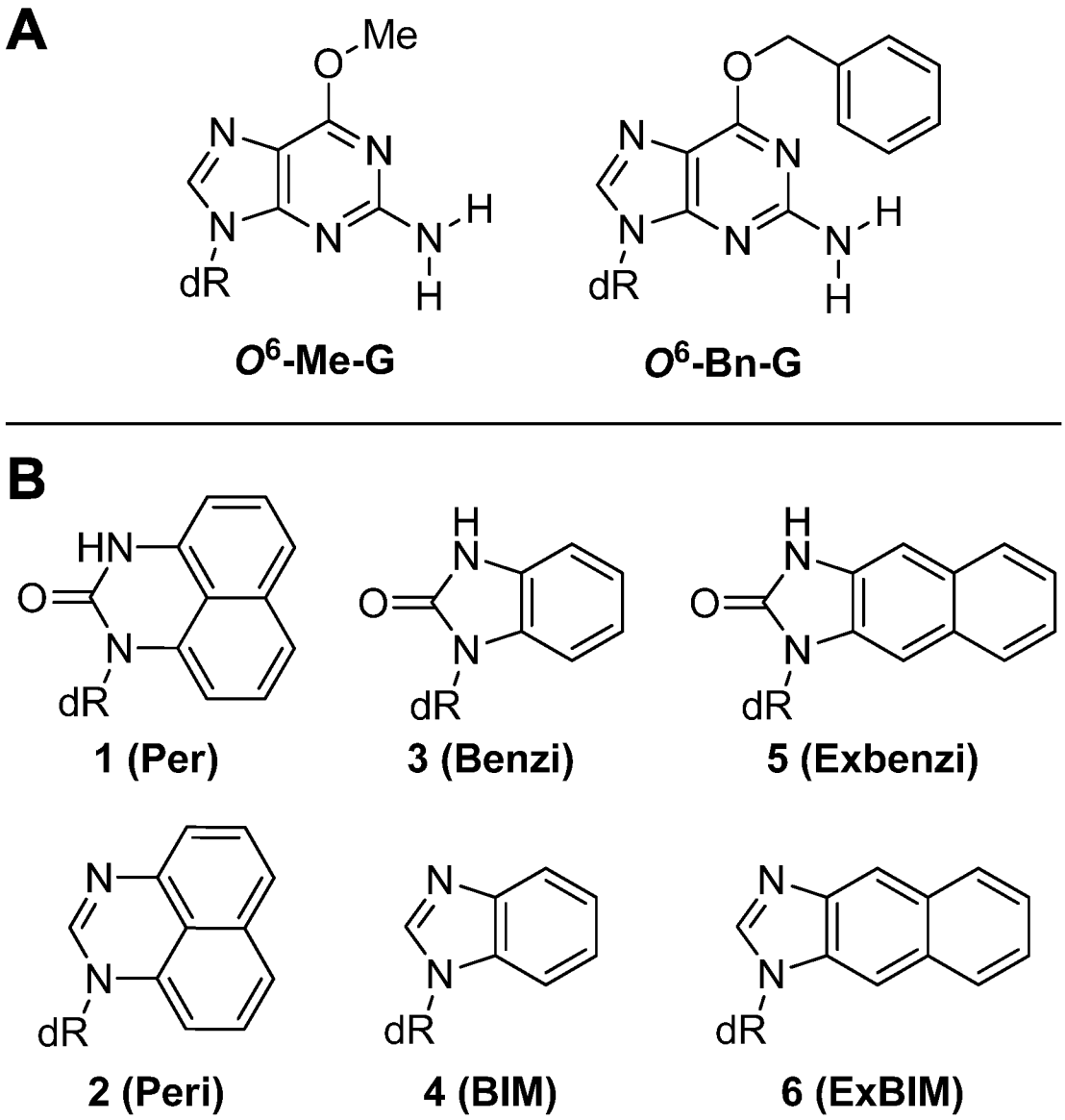
A
Me
O
N
N
N
N
H
dR
O^6-Me-G
O^6-Bn-G
B
HN
O
1 (Per)
3 (Benzi)
5 (Exbenzi)
2 (Peri)
4 (BIM)
6 (ExBIM)

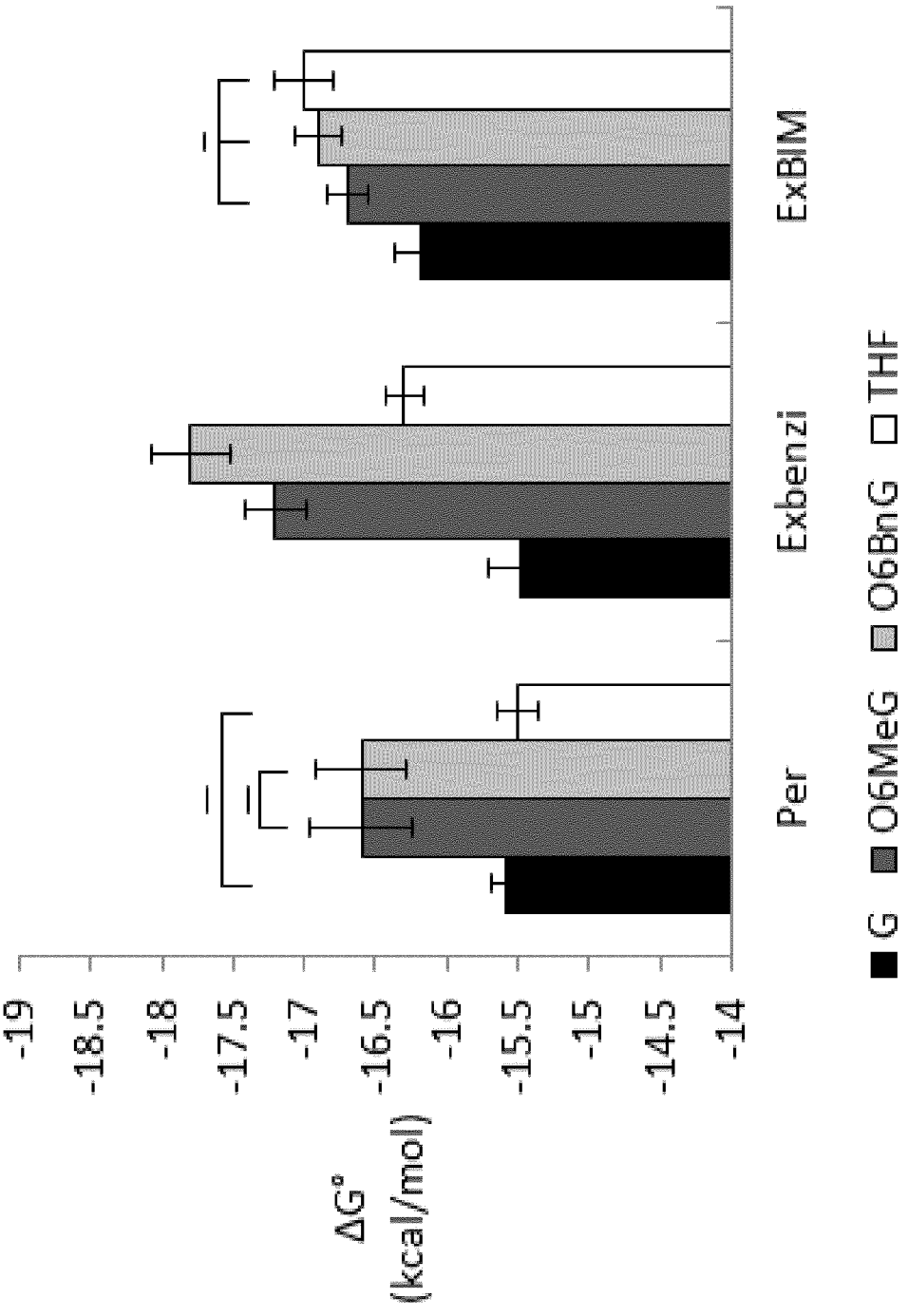
ΔG°
(kcal/mol)
-19
-18.5
-18
-17.5
-17
-16.5
-16
-15.5
-15
-14.5
-14
Per
Exbenzi
ExBIM
G
O6MeG
O6BnG
THF

Figure 2

Figure 3A

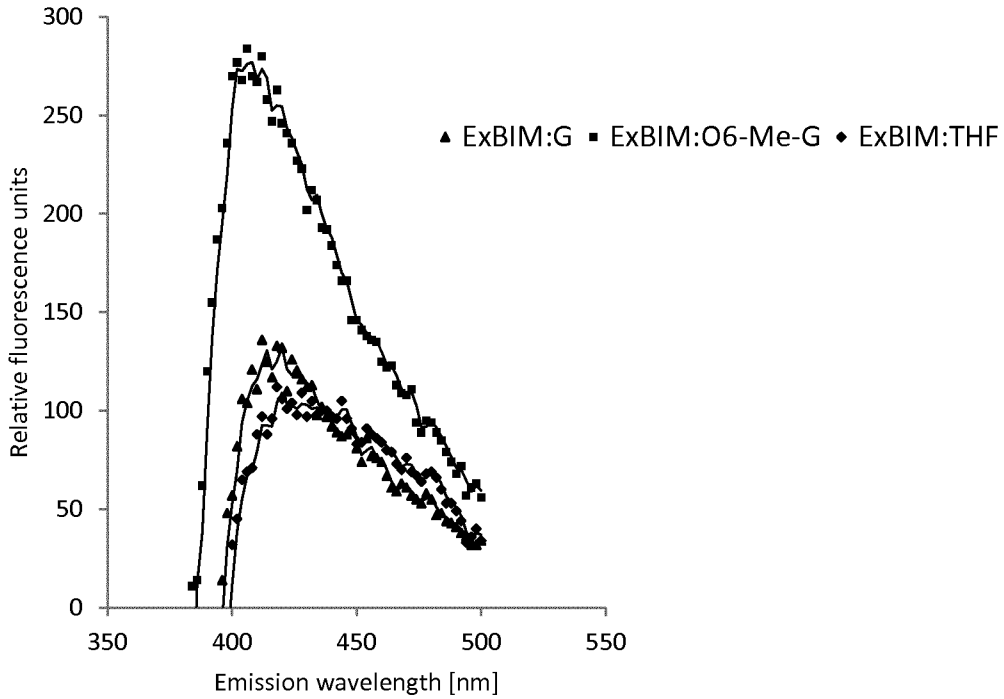

Figure 3B

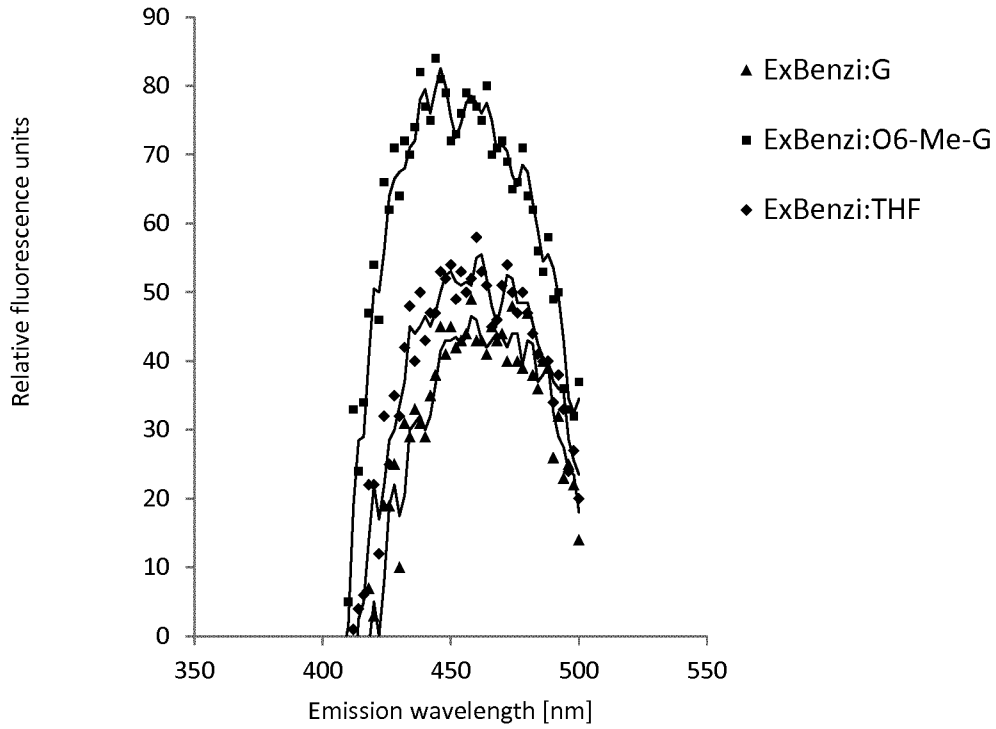

Figure 4

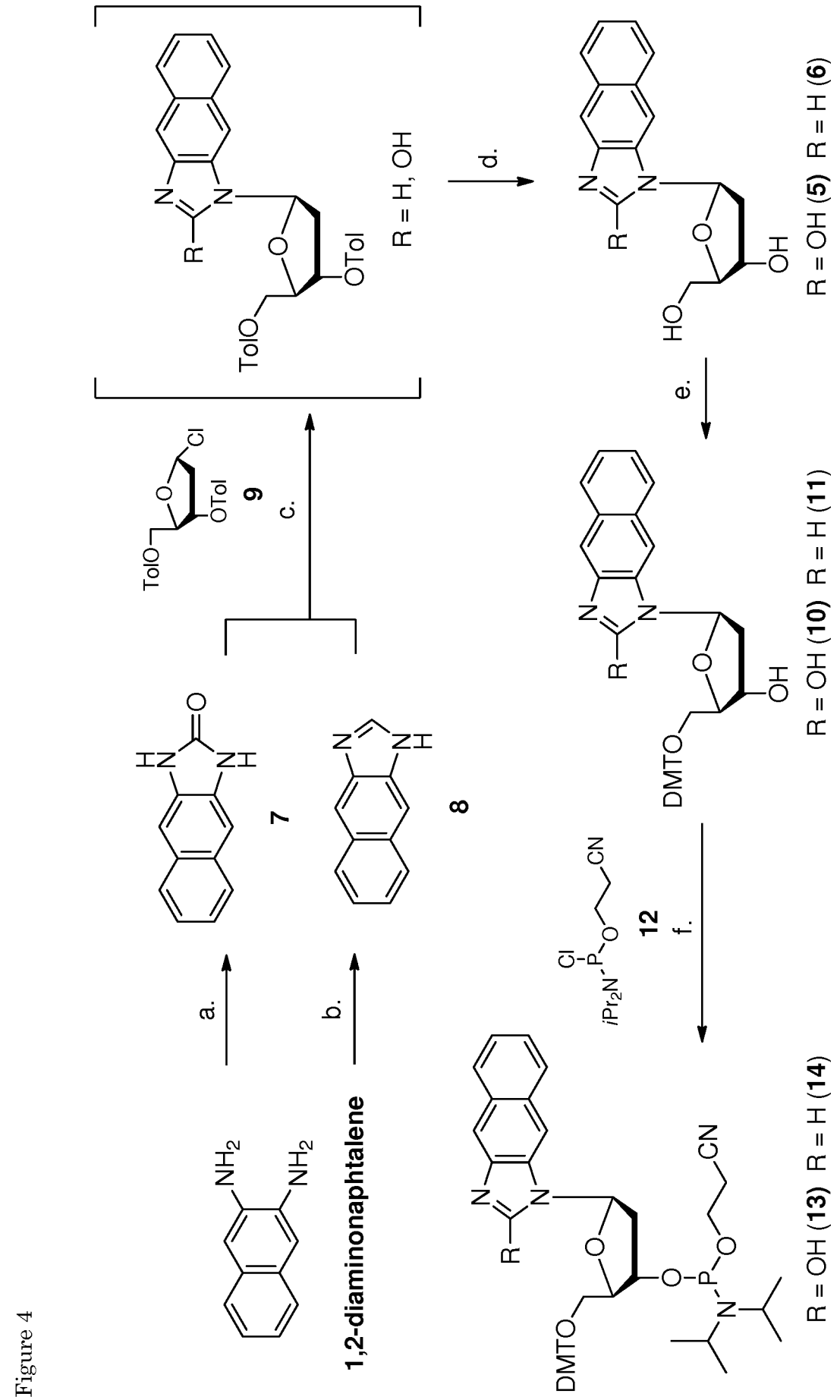
1,2-diaminonaphtalene
a.
b.
c.
d.
e.
f.
7
8
9
12
R = H, OH
R = OH (5) R = H (6)
R = OH (10) R = H (11)
R = OH (13) R = H (14)
DMTO
TolO
OTol
Cl
CN
HO
OH

Figure 5

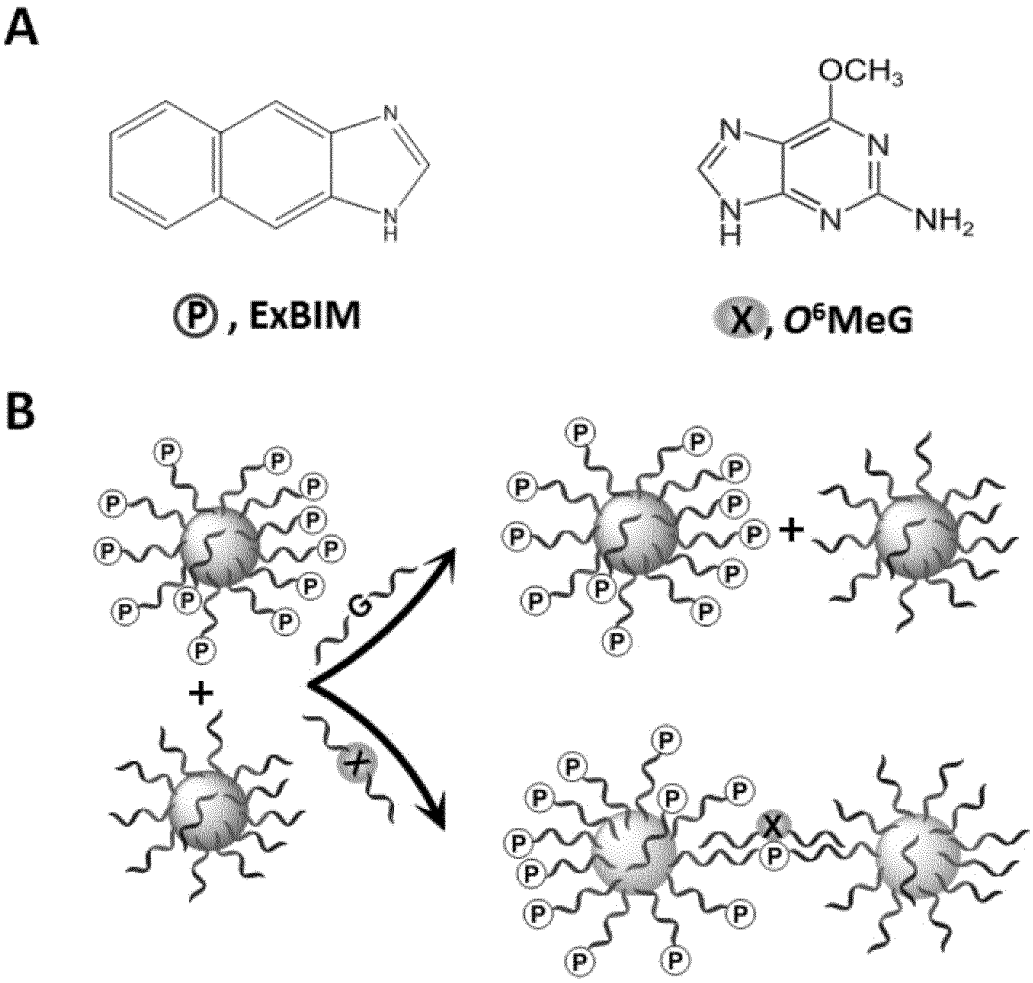

Figure 6

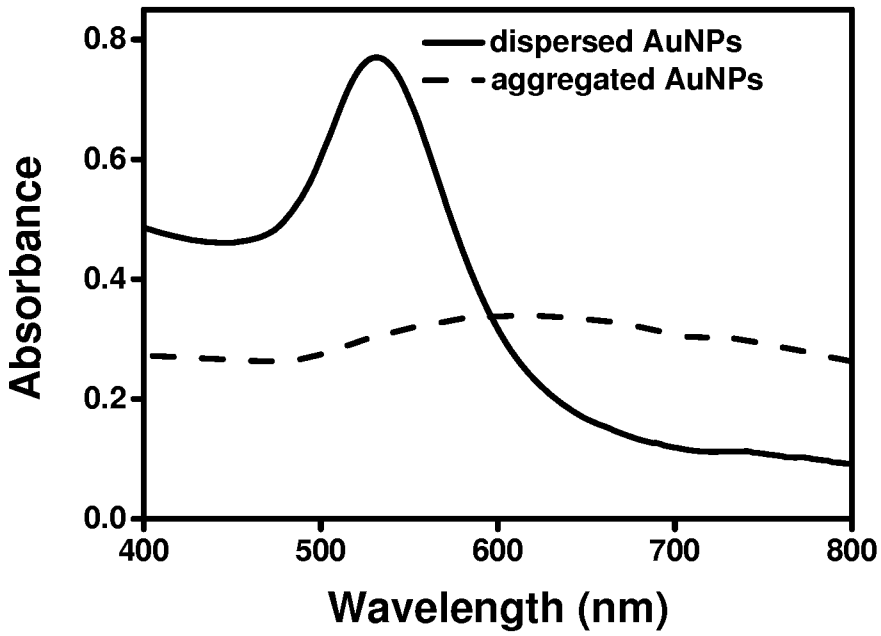
dispersed AuNPs
aggregated AuNPs
Absorbance
0.0
0.2
0.4
0.6
0.8
400
500
600
700
800
Wavelength (nm)

Figure 7

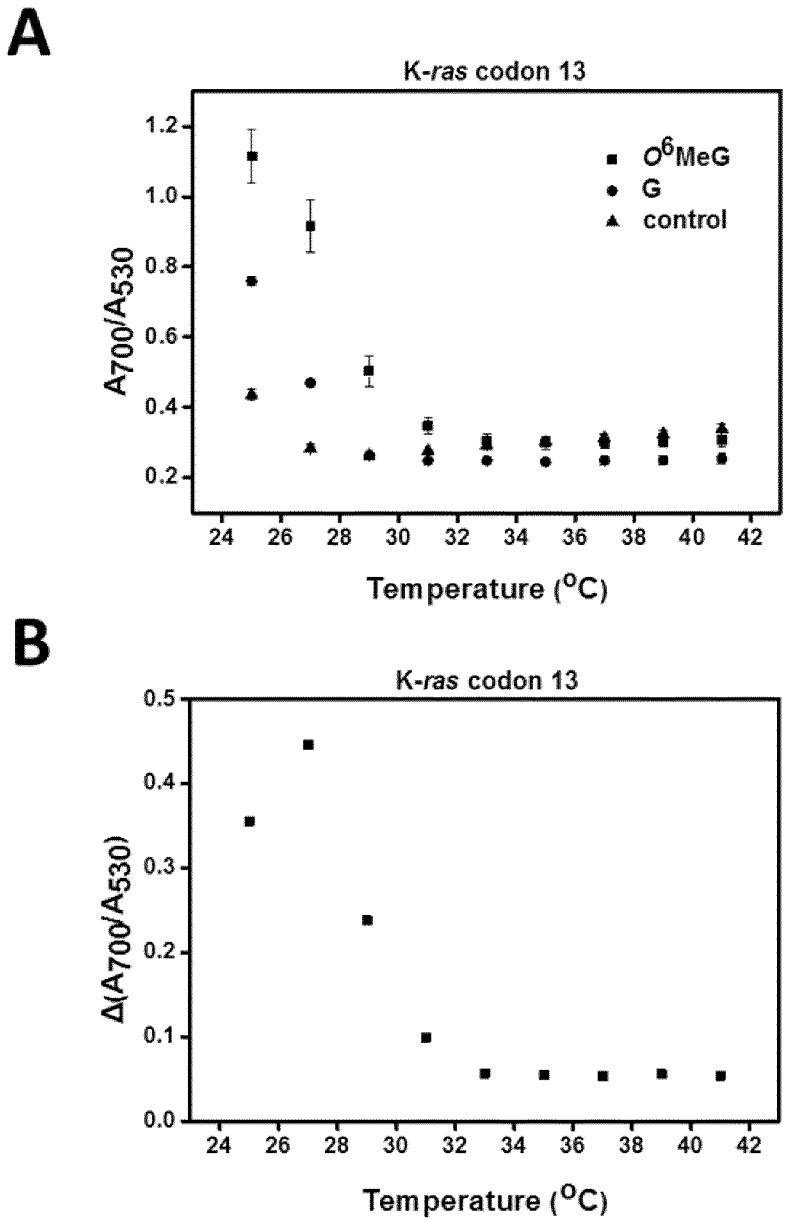
A
K-ras codon 13
O6MeG
G
control
A700/A530
Temperature (°C)
B
K-ras codon 13
Δ(A700/A530)
Temperature (°C)

Figure 8

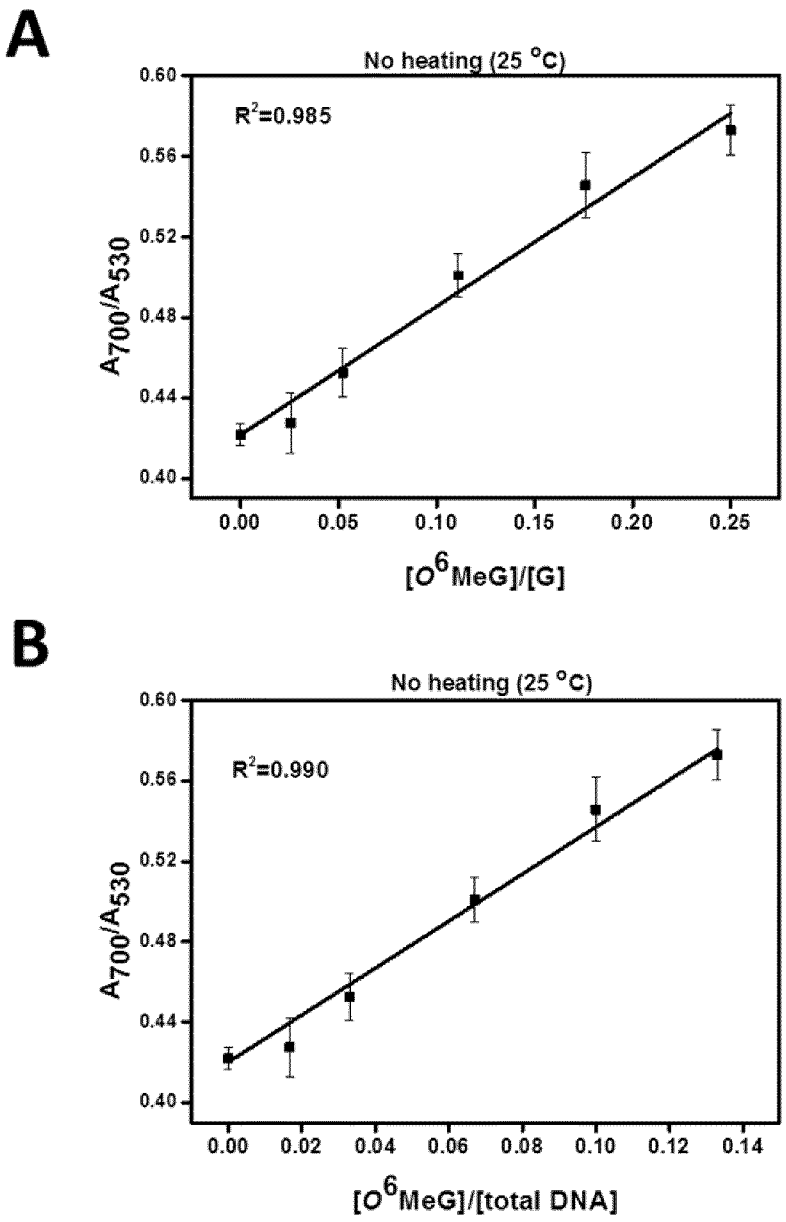
A
No heating (25 °C)
R²=0.985
A700/A530
[O6MeG]/[G]
B
No heating (25 °C)
R²=0.990
A700/A530
[O6MeG]/[total DNA]

INTERNATIONAL SEARCH REPORT

International application No
PCT/EP2015/058600

A. CLASSIFICATION OF SUBJECT MATTER
INV. C07H19/052 C12Q1/68
ADD.

According to International Patent Classification (IPC) or to both national classification and IPC

B. FIELDS SEARCHED

Minimum documentation searched (classification system followed by classification symbols)
C07H

Documentation searched other than minimum documentation to the extent that such documents are included in the fields searched

Electronic data base consulted during the international search (name of data base and, where practicable, search terms used)
EPO-Internal, WPI Data, CHEM ABS Data

C. DOCUMENTS CONSIDERED TO BE RELEVANT

Category*	Citation of document, with indication, where appropriate, of the relevant passages	Relevant to claim No.
A	JIACHANG GONG ET AL: "A Synthetic Nucleoside Probe that Discerns a DNA Adduct from Unmodified DNA", JOURNAL OF THE AMERICAN CHEMICAL SOCIETY, vol. 129, no. 16, 1 April 2007 (2007-04-01), pages 4882-4883, XP055198049, ISSN: 0002-7863, DOI: 10.1021/ja070688g the whole document	1-15

-/--

[X] Further documents are listed in the continuation of Box C.

[X] See patent family annex.

* Special categories of cited documents :

"A" document defining the general state of the art which is not considered to be of particular relevance

"E" earlier application or patent but published on or after the international filing date

"L" document which may throw doubts on priority claim(s) or which is cited to establish the publication date of another citation or other special reason (as specified)

"O" document referring to an oral disclosure, use, exhibition or other means

"P" document published prior to the international filing date but later than the priority date claimed

"T" later document published after the international filing date or priority date and not in conflict with the application but cited to understand the principle or theory underlying the invention

"X" document of particular relevance; the claimed invention cannot be considered novel or cannot be considered to involve an inventive step when the document is taken alone

"Y" document of particular relevance; the claimed invention cannot be considered to involve an inventive step when the document is combined with one or more other such documents, such combination being obvious to a person skilled in the art

"&" document member of the same patent family

Date of the actual completion of the international search	Date of mailing of the international search report
25 June 2015	08/07/2015

Name and mailing address of the ISA/	Authorized officer
European Patent Office, P.B. 5818 Patentlaan 2 NL - 2280 HV Rijswijk Tel. (+31-70) 340-2040, Fax: (+31-70) 340-3016	Gavriliu, Daniela

INTERNATIONAL SEARCH REPORT

International application No
PCT/EP2015/058600

C(Continuation). DOCUMENTS CONSIDERED TO BE RELEVANT

Category*	Citation of document, with indication, where appropriate, of the relevant passages	Relevant to claim No.
Y	H.L.GAHLON; S.J.STURLA: "Hydrogen Bonding or Stacking Interections in Differentiating Duplex Stability in Oligonucleotides Containing Synthetic Nucleoside Probes for Alkylated DNA", CHEM. EUR. J., vol. 19, 2013, pages 11062-11067, XP002741399, the whole document	1-15
A	HIJAZI ABDULLAH ET AL: "Nucleosides. XL. Synthesis and properties of lin-naphthimidazole- ribonucleosides", NUCLEOSIDES & NUCLEOTIDES, MARCEL DEKKER INC, US, vol. 3, no. 5, 1 January 1984 (1984-01-01) , pages 549-557, XP009102041, ISSN: 0732-8311, DOI: 10.1080/07328318408081289 the whole document	1-15
Y	WO 2004/031405 A1 (ECOLE POLYTECH [CH]; KINDERMANN MAIK [CH]; JOHNSSON KAI [CH]; BIERI CH) 15 April 2004 (2004-04-15) claims; figures; examples	1-15
Y	WO 94/12517 A1 (ANTIVIRALS INC [US]) 9 June 1994 (1994-06-09) claims; figures; examples	1-15
Y	ZHIJIAN ZHU ET AL: "Design, Synthesis, and Biological Evaluation of Tricyclic Nucleosides (Dimensional Probes) as Analogues of Certain Antiviral Polyhalogenated Benzimidazole Ribonucleosides", JOURNAL OF MEDICINAL CHEMISTRY, vol. 43, no. 12, 1 June 2000 (2000-06-01), pages 2430-2437, XP055198414, ISSN: 0022-2623, DOI: 10.1021/jm990290y chart 1	1-15

INTERNATIONAL SEARCH REPORT

Information on patent family members

International application No
PCT/EP2015/058600

Patent document cited in search report	Publication date	Patent family member(s)	Publication date
WO 2004031405 A1	15-04-2004	AU 2003271669 A1	23-04-2004
		CA 2501063 A1	15-04-2004
		CN 1720332 A	11-01-2006
		EP 1546371 A1	29-06-2005
		JP 4976651 B2	18-07-2012
		JP 2006501289 A	12-01-2006
		KR 20050062588 A	23-06-2005
		NZ 538986 A	30-06-2006
		US 2006024775 A1	02-02-2006
		WO 2004031405 A1	15-04-2004
		ZA 200502210 A	22-02-2006
WO 9412517 A1	09-06-1994	AU 676704 B2	20-03-1997
		CA 2149765 A1	09-06-1994
		EP 0669927 A1	06-09-1995
		JP H08506093 A	02-07-1996
		US 5405938 A	11-04-1995
		WO 9412517 A1	09-06-1994